Received: 13 December 2019 | Revised: 14 February 2020 | Accepted: 17 February 2020

DOI: 10.1002/wsbm.1485

ADVANCED REVIEW

WIREs SYSTEMS BIOLOGY AND MEDICINE WILEY

Multiscale modeling of vertebrate limb development

Tilmann Glimm[1] | **Ramray Bhat**[2] | **Stuart A. Newman**[3]

[1]Department of Mathematics, Western Washington University, Bellingham, Washington

[2]Department of Molecular Reproduction, Development and Genetics, Indian Institute of Science, Bangalore, India

[3]Department of Cell Biology and Anatomy, New York Medical College, Valhalla, New York

Correspondence
Tilmann Glimm, Department of Mathematics, Western Washington University, Bellingham, WA 98229.
Email: glimmt@wwu.edu

Abstract

We review the current state of mathematical modeling of cartilage pattern formation in vertebrate limbs. We place emphasis on several reaction–diffusion type models that have been proposed in the last few years. These models are grounded in more detailed knowledge of the relevant regulatory processes than previous ones but generally refer to different molecular aspects of these processes. Considering these models in light of comparative phylogenomics permits framing of hypotheses on the evolutionary order of appearance of the respective mechanisms and their roles in the fin-to-limb transition.

This article is categorized under:
Analytical and Computational Methods > Computational Methods
Models of Systems Properties and Processes > Mechanistic Models
Developmental Biology > Developmental Processes in Health and Disease
Analytical and Computational Methods > Analytical Methods

KEYWORDS

BMP, fin-limb transition, galectin, Turing-type mechanism, Wnt

1 | INTRODUCTION

The formation of the precursors of the skeletal elements in vertebrate limbs is one of the best-studied examples of pattern formation in developmental biology (Mariani & Martin, 2003; Newman, Glimm, & Bhat, 2018; Tickle, 2003). The arrangement of skeletal elements of limb bones is well conserved across the tetrapods, with a characteristic increase in the number of elements in the proximal–distal direction (Figure 1, upper box, left). These skeletal elements are preceded by cartilaginous templates, which in turn arise from tight aggregates of mesenchymal cells known as precartilage condensations. Anticipating the appearance of the skeleton, patterns of precartilage condensations in amniotes (reptiles, birds, and mammals) emerge proximodistally as well, although some amphibian species are exceptions to this. In most tetrapod species, the cartilaginous template of the limb skeleton is eventually replaced by bone.

Remarkably, the patterned condensation of limb mesenchyme also occurs in vitro (Ahrens, Solursh, & Reiter, 1977; De Lise, Stringa, Woodward, Mello, & Tuan, 2000). Mesenchymal cells, when isolated from developing chicken or mouse limbs, dissociated and cultured as high-density "micromasses," form spots or labyrinthine stripe-like structures within about a day of plating (Christley, Alber, & Newman, 2007; Downie & Newman, 1994; Kiskowski et al., 2004). Randomized, reaggregated mesenchymal cells also generate separated cartilaginous elements when packed into a limb bud ectodermal jacket (Ros, Lyons, Mackem, & Fallon, 1994; Zwilling, 1964). It is thus widely accepted that the in vitro condensation process is equivalent to, and recapitulates mechanisms of differentiation and pattern formation seen in, the in vivo process. In particular, precartilage condensation of limb mesenchyme takes place in the absence of signals from the limb bud ectoderm such as the Fibroblast Growth Factor (FGF-8)-producing apical ectodermal ridge (AER), and the specialized Sonic Hedgehog (Shh)-producing region of mesenchyme at the limb bud's posterior junction with the body wall, the zone of polarizing activity (ZPA).

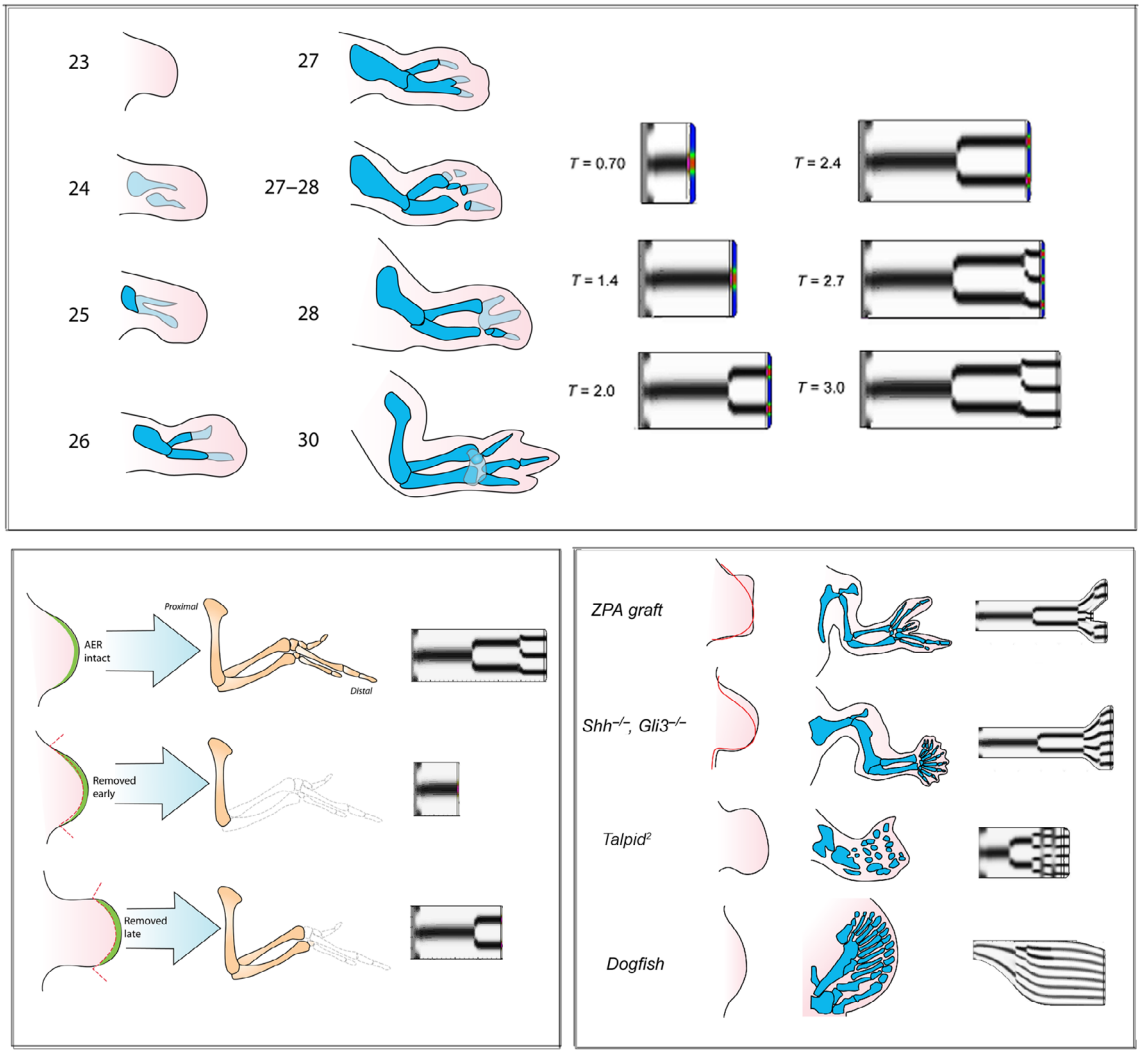

FIGURE 1 Depictions of the development of normal, experimentally manipulated, and mutant limbs, and of simulations with the TFF model. (Upper box, Left) Proximodistal developmental progression of chicken forelimb between days 3 and 7 of development (indicated by the corresponding Hamburger–Hamilton stages [Hamburger & Hamilton, 1951]). Early cartilage, including precartilage condensations, shown in light blue; definitive cartilage shown in darker blue. (Right) A series of snapshots from the simulation of normal limb development by the discontinuous Galerkin FEA method (Zhu, Zhang, Alber, & Newman, 2010), using the morphostatic reduction (Alber et al., 2008) of the TFF model of Hentschel, Glimm, Glazier, and Newman (2004). (Lower left box) Simulations of AER removal based on the TFF–FEA model. (Left columns) Drawings of AER removal experiments (Saunders, 1948). Top images show an intact chicken wing bud at an early stage of development and the limb skeleton that it generates. Middle images show an early stage wing bud with the AER removed, and the resulting limb skeleton, which develops normally but is truncated at the elbow. Bottom images show a later stage wing bud whose AER has been removed. The resulting skeleton is truncated from the wrist onward. (Right column) Simulations of limb development as in upper box. (Top) AER (i.e., the source of suppressive FGF morphogen) active throughout simulation; normal development results. (Middle) AER turned off early during the simulation. (Bottom) AER deleted later during the simulation. All simulations ran for the same duration. (Lower right box) TFF–FEA simulations of effect of distal expansion of developing limb. (Top row, left column) Drawing of expanded chicken wing bud resulting from anterior graft of an ectopic ZPA from another wing bud (normal limb profile at this stage shown in red); (Top row, center column) resulting cartilage skeleton, with mirror-image duplication; (Top row, right column) End-stage of simulation with distally expanded limb bud corresponding to that shown on left. (Second row, left column) Expanded mouse forelimb bud in embryos null for both Shh and Gli3 (normal limb profile at this stage shown in red); (Second row, center column) Resulting skeleton, with supernumerary digits (Litingtung, Dahn, Li, Fallon, & Chiang, 2002); (Second row, right column) End-stage of simulation with distal expansion corresponding to that shown on left. (Third row, left column) Expanded wing bud of chicken embryo homozygous for *talpid*^{2} mutation; (Third row, center column) Cartilage skeleton formed from such a limb bud later during development; (Third row, right column) End-stage of simulation with distal expansion corresponding to that shown on left. (Bottom row, left column) Shape of the pectoral fin-bud in an embryo of the dogfish *Scyliorhinus torazame*; (Bottom row, center column) Cartilaginous fin skeleton formed from such a limb bud; (Bottom row, right column) End-stage of simulation using a limb bud contour like that shown on left. Source: Figures adapted from Zhu et al. (2010), which should be referred to for additional details. AER, apical ectodermal ridge; FEA, finite element analysis; FGF, Fibroblast Growth Factor; TFF, TGF-β, fibronectin, and FGF model; ZPA, zone of polarizing activity

Limb bud mesenchyme thus has an inherent self-organizing capacity, which leads to the spontaneous formation of patterns. This has a number of consequences for modeling skeletal pattern formation. First, the basic mechanisms of precartilage condensation may be studied independently of cell division and directed movement associated with the growth process of the limb. Second, these basic mechanisms are also independent of positional information (PI) encoded by morphogen and other gradients that emanate from signaling/inducing centers. But while growth is not required for the formation of condensations, the asymmetrical proximodistal patterning of the resulting skeletal elements is dependent on limb bud elongation. Moreover, gradients of morphogens such as FGFs and Shh and those of transcription factors encoded by Hox-, Gli-, Hand-, and Msx-family genes play important roles in refining and sculpting the condensations laid out by the inherent self-organizing mechanism of limb mesenchyme.

We review mathematical models of limb chondrogenesis in this survey. These fall into two broad categories: (a) mechanical or mechanochemical models, where it is the mechanical properties of the cells or the extracellular matrix (ECM) that lead to pattern formation (e.g., Oster, Murray, & Harris, 1983; Zeng, Thomas, Newman, & Glazier, 2002); (b) reaction–diffusion (RD)-type models (such as those described in a seminal paper by the mathematician Alan Turing [Turing, 1952], but where both "reaction" and "diffusion" are given cell biological interpretations [Newman, 2007]); here the interplay of two or more secreted molecules sets up a prepattern of concentrations that serves as the template for the condensations (e.g., Hentschel et al., 2004; Newman & Frisch, 1979; Raspopovic, Marcon, Russo, & Sharpe, 2014). The PI concept, in which patterns are determined by the "readout" of spatial or temporal gradients of morphogens by sophisticated cellular programs (Wolpert, 1969), has rarely been modeled mathematically without reference to mechanisms from the other categories (but see, e.g., Woolley, Baker, Tickle, Maini, & Towers, 2014).

These categories of mechanism are clearly not mutually exclusive. In fact, they often work in concert to generate patterns. For example, the model of Glimm, Bhat, and Newman (2014) combines aspects of (a) and (b). In addition, if prepatterns of condensations are laid out via a Turing-type mechanism (Turing, 1952), there is still the requirement of translating this prepattern into the actual pattern, which must involve directed cell motion, likely mediated by the interplay of the physical properties of the cells and the chemical prepatterns. In other words, downstream from a Turing-type patterning module, a mechanochemical module is required to lock in the patterns.

These mechanisms can work in sequence during development, whereby a chemical pattern, either via an RD mechanism or PI-imparting gradient, is established first, followed by a mechanical morphogenetic response, or simultaneously, wherein chemical and mechanical processes act in concert. These have been schematized, respectively, as "morphostatic" and "morphodynamic" compound patterning mechanisms (Salazar-Ciudad, Jernvall, & Newman, 2003).

Elements specified by RD and mechanochemical processes are typically repeating modules, but actual repetitive skeletal elements (e.g., the radius and ulna, the individual digits) are generally different from one another morphologically. This implies the existence of mechanisms that impart this specificity. Spatial heterogeneities in molecular expression and secretion within the limb mesoderm (e.g., Hox protein, FGF, or Shh gradients) prior to its patterning could (as in the original PI hypothesis) determine both the positions and identities of elements. Alternatively, they could provide nonuniform conditions that individualize the outcomes of more generic periodicity generating (e.g., RD) processes (Newman, 1988; Stewart, Bhat, & Newman, 2017). A schematic diagram of the categories of models discussed in this review is provided in Figure 2.

Lastly, the evolutionary relationships of the endoskeletons of tetrapod limbs and fish fins create a presumptive ordering among the hypothesized mechanisms underlying their repetitive spacing patterns. In particular, Turing-type mechanisms or their hybrid mechanochemical counterparts, which naturally form structures with intrinsic spatial periodicity, appear more fundamental, phylogenetically and embryologically, than PI mechanisms, which arise from no such inherent propensities, and whose function may be an evolutionary refinement (Newman et al., 2018).

The past three decades have seen several reviews and critical discussions of mathematical models of limb skeletogenesis (e.g., Chaturvedi et al., 2005; Glimm, Headon, & Kiskowski, 2012; Iber & Zeller, 2012; Maini & Solursh, 1991; Marcon, Diego, Sharpe, & Muller, 2016; Newman & Bhat, 2007; Newman & Müller, 2005; Woolley et al., 2014; Zhang, Alber, & Newman, 2012). Based on the more recent experimental and theoretical efforts described above, the models that we will discuss in the remainder of this review, start from the observation that limb chondrogenesis is a *self-organizing process*, which produces patterns with an inherent *periodicity* that is remarkably *robust*. Specifically, it is the interplay of inherent morphogenetic properties of limb mesenchyme (self-organization) with long-range mechanisms most commonly mediated by morphogens that organizes these local properties into a global pattern-forming process with a characteristic wavelength (spatial periodicity). Robustness and phenotypic specificity are attained by

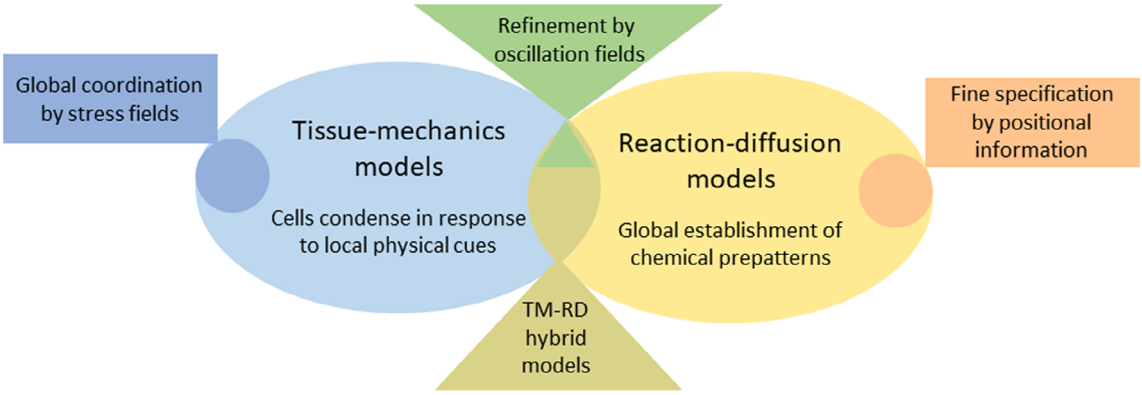

FIGURE 2 Venn diagram of the categories of models discussed in this review. The main models involve (a) local self-organization of mesenchymal cells into precartilage condensations (e.g., Zeng et al., 2002; Zeng, Thomas, & Glazier, 2004), or variations of this *tissue mechanics* scheme in which tensile forces due to long-range organization of the ECM influence the global character of the patterns (e.g., Oster et al., 1983); (b) interactions of morphogen production and transport leading to chemical patterns for eventual placement of condensations (e.g., Badugu, Kraemer, Germann, Menshykau, & Iber, 2012; Hentschel et al., 2004; Newman & Frisch, 1979; Raspopovic et al., 2014), or variations of this *reaction-diffusion* scheme in which the specific characters of patterned skeletal elementsare influenced by monotonic PI gradients (e.g., Glimm, Zhang, Shen, & Newman, 2012; Raspopovic et al., 2014); and (c) mechanisms in which tissue mechanics and RD effects interact in a morphodynamic fashion (sensu Salazar-Ciudad et al., 2003) in the generation of skeletal elements (e.g., Glimm et al., 2014; Oster, Murray, & Maini, 1985) or variations on this *hybrid* scheme in which coordination and refinement of skeletal elements is effected by global synchronization of cellular oscillators (Glimm et al., 2019). ECM, extracellular matrix; PI, positional information; RD, reaction–diffusion; TM, tissue mechanics

consolidation and reinforcement of the basic chondrogenic mechanism through other processes that evolved from independent mechanisms.

2 | INHERENT MORPHOGENETIC AND PATTERN-FORMING PROPERTIES OF LIMB MESENCHYME

Limb patterning models that focus on the inherent capacity of the limb mesenchyme to undergo condensation can be strictly local, in the sense that they are based on interactions of the cells with their immediate surrounding, or global, in the sense that there are long-range signals that coordinate cell behavior. Global coordination, which appears to be essential for the regular pattern formation observed in limb and fin endoskeleton formation and in limb bud-derived micromass cultures, can be achieved by nonlocal mechanical effects such as traction on the surrounding ECM (Oster et al., 1983), or by diffusible chemical signals, that is, morphogens, as in RD models discussed below.

In some of the models we describe, mechanical properties of the limb mesenchyme such as random cell motion in conjunction with cell-cell adhesion or cell-matrix adhesion, or mechanical properties of the ECM provide the core mechanism of pattern formation. In other models, long-range chemical signals (morphogens) are crucial for the establishment of patterns. In the latter category, the establishment of patterns in the morphogen concentrations could either happen independently of cell movement (the "morphostatic" case according to a classification by Salazar-Ciudad et al. (2003) or together with cell movement as an indispensable component ("morphodynamic"). These fall into the broad category of lateral activation and local inhibition (LALI) models, the most frequently employed extensions of Turing's RD mechanism (Turing, 1952).

2.1 | Mechanical and mechanochemical models

Several models based only on local adhesion of mesenchymal cells have been proposed. Zeng et al. (2002) formulated a model in which the ECM molecule fibronectin plays a central role. (See also Zeng et al., 2004.) Fibronectin is produced by the mesenchymal cells and does not diffuse in the matrix. It mediates cell-matrix adhesion and is found in high concentrations within precartilage condensations. In the model of Zeng and coworkers, cells undergo random walks that are biased due to cells adhering more strongly to fibronectin-rich than fibronectin-poor regions of the matrix, resulting

in movement up gradients of fibronectin. Cells thus get "trapped" in regions of high fibronectin concentration; since they produce fibronectin themselves, there is a positive effective feedback, which causes the aggregation of cells and spacing of aggregates.

Using the Cellular Potts Model, a cellular automata framework, the authors simulated this mechanism and found that it indeed produced patterns of cell aggregates. The topology depended on the cell density, with low cell density leading to spot-like patterns, and higher cell density to labyrinthine and stripe-like patterns. It is notable that the proposed mechanism is a purely local one, with no diffusible morphogen or other long-range mechanism for coordinating the local behavior. Correspondingly, the characteristic wavelength of the patterns that form is not constant in time, but increases as condensations coalesce, a process that continues until all cells become incorporated in condensations and coalescence terminates. This is in contrast to experimental results, where there is very little coalescence of condensations and the typical wavelength of the pattern does not change much in time from the initial establishment of the pattern, although some coalescence does occur (Downie & Newman, 1994). Quantitative evidence for a characteristic pattern wavelength (albeit a noisy one) in vitro (Kiskowski et al., 2004; Christley et al., 2007), a self-organizing property of the limb mesenchyme presumed to also pertain to the embryonic setting, suggests that purely local mechanisms of condensation patterning are insufficient to account for skeletogenesis.

Mochizuki, Wada, Ide, and Iwasa (1998) showed that mixed cultured cells taken from two different stages of avian limb development (stages 20 and 24) will sort into clusters of cells from the same stage, forming aggregates that resemble in vitro chondrogenic condensations. This is analogous to other cell sorting experiments that have been explained by the differential adhesion hypothesis (Glazier & Graner, 1993; Steinberg, 2007) and strongly indicate that the cells from the different stages differ in adhesive properties (see also Yokouchi et al., 1995, discussed in Newman, 1996). This in turn could mean either that cells at different stages produce different adhesion molecules, or that there is a temporal monotonic increase in the abundance of some adhesion molecule. Mochizuki et al. showed that simple computer simulations based on such differential adhesion assumptions could quantitatively reproduce the experimental results. It is important to note that these experiments did not establish a definite mechanism of prechondrogenic condensation in vivo or in vitro since the authors' experiments indicate that mixtures of two different cell cultures from the same stage of development do not sort. Still, the results indicate that cell-cell adhesive properties change throughout the formation of precartilage condensations, and thus likely play some role in this formation.

Earlier, in the 1980s, Oster, Murray and coworkers developed several related models for limb chondrogenesis in which the interaction of the cells with the mechanical properties of the ECM plays a crucial role. The first of these, described in Oster et al. (1983), is a purely mechanical model based on the observations that motile cells can generate large traction forces on fibrous ECMs, and that cells undergo haptotaxis, that is, move up adhesive gradients in their substratum. This leads to effective movement up the gradients of ECM density. The authors set up a system of partial differential equations (PDEs) which included as variables the cell density, the ECM density and the local matrix velocity, describing the displacement of the ECM. Correspondingly, there are three equations required for the model: spatiotemporal evolution equations for the cell density and the ECM density, as well as a force balance equation. This latter equation encapsulates the assumption that the entire tissue is always in mechanical equilibrium. This means that any force generated locally by cell traction or cell shape change instantaneously equilibrates across the tissue.

While the model of Oster, Murray, and Harris is a purely mechanical one that does not consider the role of long-range cell–cell communication in regulating the composition of the ECM, it differs from the purely local model of Zeng and coworkers (see above). Specifically, aggregation resulting from an interplay of the quasi-local phenomenon of cells moving by haptotaxis while deforming the ECM can be considered as part of a more general framework of local interactions within an imposed globally coordinating mechanism. The fact that the whole material is assumed to be in mechanical force equilibrium means that such local deformations are effectively globally coordinated. A problem with this model is that the globally acting aspect, deformation of the matrix, is based on experiments on cells in fibrous type I collagen lattices (Harris, Stopak, & Warner, 1984; Harris, Stopak, & Wild, 1981). The ECM of the precondensed limb mesenchyme, in contrast, is a gel of glycosaminoglycans and nonfibrous glycoproteins that lacks the long-range organization of collagenous matrices.

A second, related model was proposed by Oster, Murray, and Maini two years later (Oster et al., 1985). In contrast to the previous purely mechanical model, this model considers the local deformation of the ECM due to the osmotic swelling of certain components of the ECM and thus falls under the category of *mechanochemical* models. This swelling, in turn, is controlled by gene products that the cells secrete. Specifically, hyaluronan or hyaluronic acid (HA), a glycosaminoglycan, causes osmotic swelling, whereas the enzyme hyaluronidase (HAase) degrades HA and thus causes deswelling of the ECM. The formal model consists of a system of PDEs that describe the interplay of cells, ECM, HA,

and HAase. Here, secreted HAase leads to deswelling of the ECM, thus causing an effective convective flux of the cells toward sites of cell aggregations. The increased cell density, in turn, induces increased secretion of HAase, and thus further deswelling.

The authors performed a mathematical analysis under certain simplifying assumptions, which shows that the core mechanism of the model is of the Turing RD type, with HA and HAase taking on formal roles of morphogens (see below). Here it is essential that HA does not diffuse, but HAase does, that is, the diffusion coefficient of HA is zero, but that of HAase is nonzero. Like the model of Oster et al. (1983), there is an interplay of a local mechanism (deswelling of the ECM leading to cell aggregation) with a long-range one, in this case the diffusion of HAase through the ECM, as well as the instantaneous mechanical force equilibration. This model thus exhibits a number of interesting mechanochemical features, although more recent work on the role of HA in limb skeletogenesis suggests that it is more of a permissive factor in the timing of development than a Turing-type morphogen (Li, Toole, Dealy, & Kosher, 2007).

2.2 | Morphogen-based models

With increased knowledge of the molecular biochemistry of limb precartilage condensation formation, it has become clear that one or more morphogens play a role in the global organization of the condensation pattern in the developing limb. Furthermore, the mechanism involved likely encompasses one or more RD processes such as described by Turing in the paper in which he first introduced the term "morphogen" (Turing, 1952).

In this section, we will describe several models based on this idea, which capture processes that may have appeared at different points in the evolution of the tetrapod limb skeleton. We have suggested that these may coordinately contribute to limb development in present-day vertebrates (Newman et al., 2018). We also note, however, that the diffusion of morphogens, though sufficient to produce nonlocal patterns in limb mesenchyme, is likely inadequate to account for observed regularities on scales much larger than the chemical wavelength of the respective RD systems. One such feature is the remarkable synchrony of the appearance of condensations seen in in vitro experiments (Bhat, Glimm, Linde-Medina, Cui, & Newman, 2019). We will return to this question in a later section where we will describe a long-range mechanism for coordination and refinement of cellular pattern apparently based on intrinsic oscillatory processes in the cells of the developing mesenchyme.

2.3 | Early RD models and the TFF model

Newman and Frisch (1979) presented the first model that suggested that a Turing-type RD system generated the characteristic patterns of precartilage mesenchymal condensations in tetrapod limbs. The model was theoretical but also informed by the new finding that the ECM protein fibronectin was present in elevated levels within precartilage condensations (Lewis, Pratt, Pennypacker, & Hassell, 1978; Silver, Foidart, & Pratt, 1981; Tomasek, Mazurkiewicz, & Newman, 1982). As predicted, fibronectin eventually proved to be a mediator of the condensation process (Frenz, Akiyama, Paulsen, & Newman, 1989; Frenz, Jaikaria, & Newman, 1989). Newman and Frisch advanced the hypothesis that morphogens whose spatial distribution was the outcome of a Turing-type mechanism controlled the expression of fibronectin. A consequence of this model (which was examined only at the stationary state; Newman, Frisch, & Percus, 1988), was that the type of patterns generated depended on the geometry of the RD-permissive region at the tip of the limb bud. In particular, the gradual narrowing of the proximal-distal length of this zone, which was experimentally established to occur (Summerbell, 1976), would lead to changes of the resulting fibronectin prepatterns and could thus explain the successive growth of the number of preskeletal elements from stylopod (humerus, femur), to zeugopod (radius and ulna, tibia and fibula), to autopod (digits) (Newman & Frisch, 1979).

Newman and Frisch's model did not explicitly identify the network of interacting morphogens that regulated fibronectin, and thus the skeletal pattern. This was revisited after experimental advances in the 1980s and 1990s had identified a core of relevant gene products that satisfied the conditions of Turing's mechanism. The first of these was the discovery that transforming growth factor beta (TGF-β) is autoactivating and induces fibronectin production (Roberts et al., 1988; Van Obberghen-Schilling, Roche, Flanders, Sporn, & Roberts, 1988). Hence, TGF-β became a candidate for an activator molecule in an activator-inhibitor process (Leonard et al., 1991; Newman, 1988). While the corresponding inhibitor was not identified, there was indirect evidence for its existence. Indeed, the Fibroblast Growth Factor (FGF) receptor FgfR2 was later found to be expressed at the site of incipient condensations (Szebenyi, Savage, Olwin, &

Fallon, 1995), where upon stimulation with FGF2, it was found to mediate an inhibitory effect restricting the expansion of condensations (Moftah et al., 2002). Based on these findings, Hentschel et al. (2004) set up the following system of PDEs involving the activator TGF-β, the inferred inhibitor, and densities of cells at successive stages of differentiation, which we will refer to as the TFF model (for TGF-β, fibronectin, and FGF):

$$\nabla^2 c = \kappa^2 c,$$

$$\frac{\partial c_a}{\partial t} = \left(J_a^1 \alpha(c, c_a) + J_a(c_a)\beta(c, c_a)\right)R + D_a \nabla^2 c_a - k_a c_i c_a,$$

$$\frac{\partial c_i}{\partial t} = D_i \nabla^2 c_i - k_a c_i\, c_a + J_i(c, c_a)\beta(\mathrm{c}, \mathrm{c_a})R,$$

$$\frac{\partial R}{\partial t} = (D_{cell} - (\lambda + \lambda_2 \gamma(c, c_a))R)\nabla^2 R - \lambda_2 \frac{\partial \gamma}{\partial c_a} R^2 \nabla^2 c_a$$

$$-\lambda_2 \frac{\partial \gamma}{\partial c} R^2 \nabla^2 c + rR\left(R_{eq} - R\right) - k_{23}\gamma(c, c_a)R.$$

Here c denotes the concentration of FGFs secreted by a specialized population of cells in the AER, a process modeled by the boundary conditions; $c_a$is the concentration of TGF-β; c_i the concentration of the inhibitor, and R denotes the cell density. The above equation for R is the outcome of a more complex model, which takes into account the concentrations of different cell types, namely cells that express FGF receptor 1 (type 1), cells that express FGF receptor 2 (type 2), and cells that derive from type 2 cells, but express higher levels of the cell-ECM adhesion molecule fibronectin (type 2′). Under the assumption that cell differentiation occurs on a faster time scale than changes in the overall cell density, the densities of the three cell types were shown to be fractions of the overall cell density R, given by $\alpha(c, c_a)$, $\beta(c, c_a)$, and $\gamma(c, c_a)$, respectively. The concentration of fibronectin was assumed to be in a steady state due to fast equilibration.

Hentschel et al. numerically investigated the TFF model and showed that it could give rise to patterns that resemble the chondrogenic condensations of normal development. Alber et al. (2008) later presented a thorough mathematical analysis of these ideas. Using concepts and terminology advanced by Salazar-Ciudad et al. (2003), the authors distinguished between morphostatic and morphodynamic mechanisms of pattern formation. As described above, the key difference is that in morphodynamic mechanisms, cell movement happens at the same time as the establishment of patterns, and indeed cell motility is a crucial ingredient for patterning, whereas in morphostatic mechanisms, the establishment of chemical (pre)patterns may occur before cell motion. Once the prepatterns are established, cells respond behaviorally to give rise to patterns in the cell densities. The TFF model of Hentschel et al. (2004) is morphodynamic. However, Alber et al. (2008) (drawing justification from their earlier demonstration that smooth solutions for that system exist globally in time; Alber, Hentschel, Kazmierczak, and Newman [2005]), derived a mathematically substantiated morphostatic limit based on the assumption that cell motion is slow compared to the spatiotemporal evolution of the activator TGF-β and the inhibitor. This reduced the system to just two equations, for the activator and inhibitor concentrations (Alber et al., 2008):

$$\frac{\partial c_a}{\partial t} = D_a \nabla^2 c_a + U(c_a) - k_a c_a c_i,$$

$$\frac{\partial c_i}{\partial t} = D_i \nabla^2 c_i + \mathrm{V}(c_a) - k_a c_a c_i.$$

Here $U(c_a)$ and $V(c_a)$ are explicit functions embodying parameters of the full TFF model of Hentschel et al. (2004) under certain biologically motivated assumptions. The investigators derived conditions on the parameters for the appearance of patterns (Alber et al., 2008).

Variants of the system of Hentschel et al. (2004) were also implemented in hybrid continuous-discrete models, where the dynamics of diffusible gene products were simulated with systems of differential equations, and the cells

were modeled via a discrete cellular automaton model, the Cellular Potts Model (Chaturvedi et al., 2005; Cickovski et al., 2005). These simulations exhibited the establishment of realistic patterns of mesenchymal condensations.

Due to the high dimensionality of the system, numerical implementation of the complete TFF model is challenging. Using a state-of the art finite element approach, the discontinuous Galerkin method (Zhu, Zhang, Newman, & Alber, 2009), Zhu et al. (2010) employed the morphostatic limit system to simulate chondrogenesis in a growing domain with an imposed proximodistal gradient with FGF-like properties and showed that this could reproduce normal patterning, as well as simulate the effects of distal truncation. Moreover, Zhu et al. (2010) showed that with modifications of the system's parameters and the limb bud shapes, the system could yield in silico patterns resembling mutant and experimentally manipulated forms (Figure 1), as well as skeletal patterns from fossil limbs when plausible assumptions are made on the shapes and growth parameters of the corresponding embryonic limb buds.

2.4 | The 2GL model

Bhat et al. (2011) investigated the role of galectins, a class of sugar-binding proteins, in the early stages of chondrogenic condensations in vitro. Of the five galectins specified in the chicken genome, chicken galectin 1A (CG-1A; alternatively, Gal-1A) mediates cell–cell adhesion, while chicken galectin 8 (CG-8; Gal-8) impairs the ability of Gal-1A to do so. This group found that staining for both galectins was detectable as early as 9 hr of incubation, marking the sites of future condensations. Production of Gal-1A and Gal-8 was enhanced within condensations, increasing dramatically for about 36 hr after incubation, then rapidly decreasing. The authors found that Gal-1A and Gal-8 formed a positive feedback loop: Adding exogenous Gal-1A caused an increase in Gal-8 production and vice versa. Yet, Gal-1A and Gal-8 were found to have opposite effects on condensations. Adding Gal-1A resulted in an increase in the number of condensations. For high doses of Gal-1A, fusion of condensations was observed. In contrast, adding Gal-8 led to fewer, less defined condensations.

While the mechanism that drives this seemingly paradoxical behavior is not fully understood, Bhat et al. (2011) advanced the following hypothesis: Galectins bind to cell-membrane counterreceptors. There are two types of counterreceptors: a shared counterreceptor, which both Gal-1A and Gal-8 can bind to, and a second counterreceptor that only Gal-8 can bind to (Gal-8, being a tandem-repeat galectin, has two carbohydrate-recognition domains). The galectin feedback loop means that production of Gal-1A is under the positive control of Gal-8 and vice versa. The finding by Bhat and coworkers that cell–cell adhesion is mediated by Gal-1A provides a ready explanation of the enhancement by Gal-1A of condensations. The inhibitory effect of Gal-8 on condensations is less straightforward. Bhat et al. (2011) provided experimental evidence that Gal-8 prevents Gal-1A-mediated aggregation and interpreted this by postulating that the two galectins compete for the shared counterreceptor. Added Gal-8 binds to shared counterreceptors, which then become unavailable to Gal-1A. The expression of Gal-8 in vitro would thus lead to reduced cell–cell adhesion and fewer, more diffuse condensations.

A mathematical model by Glimm et al. (2014) implemented these assumptions. The model consists of a system of three PDEs with the cell density and the concentrations of Gal-1A and Gal-8 as variables. The counterreceptors were modeled by making the (generalized) cell density a function of the concentrations of free shared counterreceptors ℓ_1, free Gal-8 counterreceptors ℓ_8 and shared counterreceptors bound to Gal-1A or Gal-8, $c_1$and c_8^1, respectively, and the complex of Gal-8 bound to its counterreceptor c_8^1. This is analogous to the approach in structured populations models, where population density depend not only on time and space, but on additional structure variables such as age and size (Diekmann, 1999; Metz & Diekmann, 1986; Thieme, 2003). This yields the following model equations for the cell density $R\left(t,x,\ell_1,\ell_8,c_1,c_8^1,c_8^8\right)$ and the densities of diffusible Gal-1A and Gal-8, $c_1^u(t,x)$ and $c_8^u(t,x)$, respectively:

$$\frac{\partial R}{\partial t}=\mathrm{D_R}\nabla^2 R-\nabla\cdot\left(RK(c_1,R)\right)-\frac{\partial}{\partial c_1}\left(\alpha\left(c_1^u,\ell_1,c_1\right)R\right)-\frac{\partial}{\partial c_8^8}\left(\beta_8\left(c_8^u,\ell_8,c_8^1\right)R\right)-\frac{\partial}{\partial c_8^1}\left(\beta_1\left(c_8^u,\ell_8,c_8^8\right)R\right)-\frac{\partial}{\partial \ell_1}((\gamma(c_1,\ell_1)$$

$$-\beta_1\left(c_8^u,\ell_8,c_8^8\right)-\alpha\left(c_1^u,\ell_1,c_1\right))R)-\frac{\partial}{\partial \ell_8}\left(\delta(\ell_8)-\beta_8\left(c_8^u,\ell_8,c_8^1\right)R\right),$$

$$\frac{\partial c_1^u}{\partial t}=D_1\nabla^2 c_1^u+\nu\int c_8^8\,RdP-\int\alpha RdP-\pi_1 c_1^u,$$

$$\frac{\partial c_8^u}{\partial t}=D_8\nabla^2 c_8^u+\mu\int c_1 RdP-\int\beta_1 RdP-\int\beta_8 RdP-\pi_8 c_8^u.$$

Here the integrals are taken over the counterreceptor space, with $dP = d\ell_1 d\ell_8 dc_1 dc_8^8 dc_8^1$. We will refer to this as the Two-Galectin + Ligands (2GL) model.

A crucial component of the model is the Gal-1A dependent cell–cell adhesion strength. This was modeled via the adhesion flux approach by Armstrong, Painter, and Sherratt (2006). Explicitly, in the above equations, the effective cell velocity was given by:

$$K(c_1,R) = \alpha_K c_1 \int_{D_{\rho_0}} \tilde{c}_1\, \sigma\big(R(t,x+r,\tilde{\ell}_1,\tilde{\ell}_8,\tilde{c}_1,\tilde{c}_8^1,\tilde{c}_8^8)\big)\, d\tilde{P}\, \frac{r}{|r|} d^n r,$$

where σ denotes a logistic function and $n = 1$, 2, or 3 is the number of spatial dimensions. The idea is that cell–cell adhesion is mediated by c_1, the concentration of the complex of Gal-1A and its counterreceptor. The effective velocity is the outcome of an averaging process over the counterreceptor space and over a spatial n–dimensional ball D_{ρ_0} of radius ρ_0, the interaction radius (Armstrong et al., 2006). Without the adhesion-based cell movement modeled by this term, the molecular network of the 2GL is incapable of forming periodic arrays of condensations (Glimm et al., 2014). This feature, which exhibits a strongly nonlinear dependence on the parameter α_K (Figure 3, left box), specifies this mechanism as a reaction–diffusion–adhesion (rather than strictly RD) process, and thus as inherently morphodynamic by the criteria of Salazar-Ciudad et al. (2003).

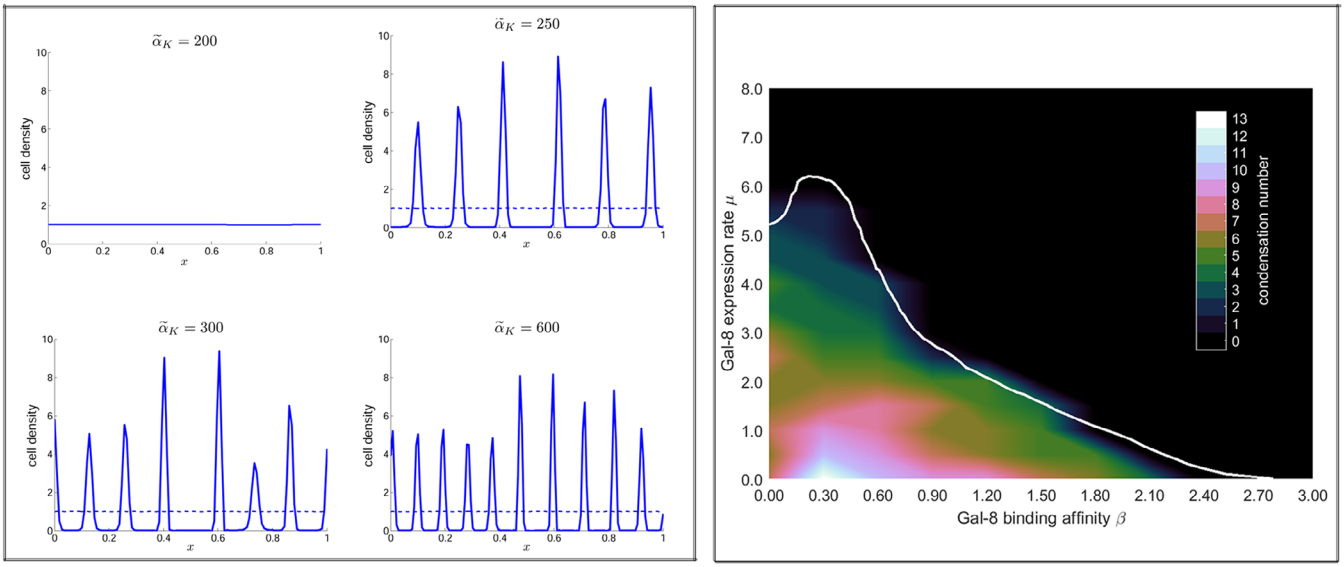

FIGURE 3 Dependence of the 2GL skeletal pattern formation model on various parameters. (Left box) Plots of the Gal-1-dependent spatial cell density for the full 2GL model at times $t = 0$ (dashed line) and $t = 1$ (solid line), for different values of the cell–cell adhesion constant α_K. For sufficiently small α_K, no spatial patterns are produced. As α_K is increased, periodic patterns appear, with an abrupt transition between $200 < \alpha_K < 250$. Further increase in α_K leads to fine-tuning of the pattern. (See Glimm et al. (2014) for details.) (Right box) Gal-8 dependence of pattern formation in the condensation-permissive parameter space of the reduced 2GL model. Two-parameter bifurcation diagram representing the dependence of condensation patterns on μ, the expression rate of Gal-8, shown on the vertical axis, and Gal-8 binding affinity β shown on the horizontal axis. A single plane of the complete parameter space is shown in which the concentration values of Gal-1 are compatible with condensation formation. According to the model, Gal-8 can participate in skeletogenic interactions with Gal-1 only if it is capable of reversibly competing with the condensation-promoting role of Gal-1. This capacity, reflected in the values of β, is a function of the primary structure of Gal-8, several residues of which in sarcopterygians have been subject to purifying selection. The expression rate of Gal-8, reflected in μ, is either constitutive or developmentally regulated, and Gal-8 genes of sarcopterygians, including the tetrapods, have acquired potential regulatory sequences for proximodistally expressed transcription factors. These could have enabled the proximodistal changes in the number of parallel elements with limb elongation seen in these species. Approximate contours demarcating the calculated number of distinct condensations are shown via a heat map within the condensation region. Source: Graph taken from Bhat, Chakraborty, Glimm, Stewart, and Newman (2016), with computations based on the model described in Glimm et al. (2014). 2GL, Two Galectin + Ligands

Together with the time dimension and n spatial dimensions, the five counterreceptor concentrations effectively lead to a $1+n+5$ dimensional problem. This can be reduced to $1+n+2$ dimensions with the assumption that counterreceptor-galectin binding happens on a faster time scale than production of proteins (Glimm et al., 2014). Still, the high dimensionality of the 2GL model by Glimm et al. (2014) along with nonlocal dynamics presents particular numerical challenges. For this reason, Glimm et al. (2014) solved the system in only one spatial dimension. They showed that for a broad range of parameters, the system is able to generate regular patterns of high and low cell density, corresponding to sites of condensations with interspersed areas of low cell density, and that increasing the initial Gal-1A concentration leads to an increase in the number of condensations. In the model, the effect of increasing Gal-8 was subtle. It was found that the percentage of unbounded shared receptors, which in turn is determined by the galectin dynamics, was a key regulatory metric. If this percentage was "high," then increasing the initial Gal-8 concentration could actually increase the wavenumber of condensations. If this percentage, however, was "low," then increasing the initial Gal-8 concentration had the opposite effect of reducing the wavenumber of the resulting pattern.

In the 2GL model, the feedback loop of the galectin dynamics sets characteristic concentrations of Gal-1A and Gal-8, which in turn determine the adhesion strength between cells. This leads, in turn, to patterns in the cell density: the cells undergo random motion and form clusters through cell–cell adhesion. As these clusters grow, their local environments are depleted of cells, which limits their sizes. This formation process falls into the broad category of LALI mechanisms (Meinhardt & Gierer, 2000). Here the role of local activation is fulfilled by cell–cell adhesion mediated aggregation, whereas lateral inhibition, rather than resulting from a diffusible inhibitor, is due to the aforementioned depletion of cell density. In the categorization outlined at the beginning of this review, however, the central role of the diffusible galectins in pattern formation provides a mechanism for global coordination of patterning.

The 2GL model can be simplified under the assumption that production of counterreceptors is much faster than the production of galectins. (This assumption would be better evaluated once the protein moieties of the sugar-bearing counterreceptors (which have proved elusive, see Grigorian & Demetriou, 2010), are experimentally identified.) The resulting equations, designated the "reduced system" (Glimm et al., 2014), are:

$$\frac{\partial \mathrm{R}}{\partial t} = \mathrm{D_R}\nabla^2 R - \nabla\cdot(R\,K(R)),$$

$$\frac{\partial c_1^u}{\partial t} = D_1\nabla^2 c_1^u + \tilde{\nu} R c_8^u - \pi_1 c_1^u,$$

$$\frac{\partial c_8^u}{\partial t} = D_8\nabla^2 c_8^u + \tilde{\mu}\left(c_1^u - \tilde{\gamma}\right)R - \pi_8 c_8^u.$$

In these equations, $R(t, x)$ is the total cell density, which just depends on time and spatial position within the limb bud or the in vitro cell mass. The "reduced" model can capture most aspects of the original model, with the exception of the subtle role of Gal-8's inhibitory effect on condensations. On the other hand, the equations are much more amenable to mathematical analysis, for example, the parameter ranges for which they can give rise to patterns can be analyzed using standard linear stability analysis (Glimm et al., 2014).

Galectin-1 and -8 have each had a complicated history of duplications and translocations during the evolution and diversification of the gnathostomes (jawed fishes) (Bhat et al., 2016; Bhat, Chakraborty, Mian, & Newman, 2014). Depending on the species, these animals contain paired fins or limbs with various arrangements of cartilaginous, or cartilage-templated, endoskeletal elements (reviewed in Newman et al., 2018). The 2GL model, having specified parameters for the expression of Gal-1 and Gal-8, their actions on cells, and their interactions with each other, affords the possibility of relating comparative properties of these proteins and the regulation of their respective genes to predicted skeletal morphologies. Some early results of this approach will be described in the section on the evolution of the limb patterning process, below.

2.5 | The BSW model

The proposal that a RD mechanism might underlie the quasi-periodic aspects of limb development (Newman & Frisch, 1979) was productively implemented by some theoretically oriented investigators (e.g., Miura & Maini, 2004; Miura

et al., 2006; Oster et al., 1985). However, this approach was largely met with skepticism by experimentalists who favored PI models (Wolpert, 1969), and in particular, the Progress Zone and ZPA models of Wolpert and his coworkers (Summerbell, Lewis, & Wolpert, 1973; Tickle, Summerbell, & Wolpert, 1975). A number of experimental findings, however, cast doubt on the validity of the progress zone and ZPA models (Chiang et al., 2001; Dudley et al., 2002; Newman, 2007; Saunders, 2002), and more than three decades after the approach was initiated, a paper by Sheth et al. (2012) using genetic manipulations refocused the interest of experimentalists on RD models for chondrogenesis. A compelling aspect of the new work was experimental evidence that the characteristic periodic patterning in the autopod of mouse embryos is due to a Turing-type mechanism.

One of the key features of the Turing mechanism is that the wavelength of the generated patterns depends on the parameters of the reaction kinetics. Thus, change in these parameters will modify the characteristic wavelength of the pattern. For instance, for a generic activator–inhibitor system producing stripes in a fixed spatial domain, continuous increase of the production rates of the activator may increase the number of stripes in a stepwise fashion. (See, e.g., the discussion of the dispersion relation of a Turing RD pattern in Murray, 2002, or the "Saunders number" in Newman & Frisch, 1979.)

Thus, in a pattern-forming system based on a Turing-type mechanism, perturbation of the reaction kinetics should modulate the pattern's wavelength. In the context of digit formation in vertebrates, this means that certain perturbations should change width and spacing of the elements in a quasi-continuous way, but with predictably abrupt consequences beyond some parameter thresholds. They would thus alter the number of digits that form in a limb bud of fixed width. Since the number of digits is a remarkably robust character for each species, this has often been raised as an argument against a Turing mechanism. Remarkably, Sheth and coworkers showed that modifications of the Hox genes in mice produced just such changes in wavelength of the patterns of chondrogenic condensations. Specifically, they created mutants in the distal Hox genes Hoxa13 and Hoxd11-1, in mice that lacked one or both copies of Gli3, a transcription factor involved in controlling the width of the limb bud (see below).

The effect on the number of digits at stage E12.5 or E13.5 was addressed by plotting the expression of the transcription factor Sox9, an early marker of chondrogenesis in mice. While previous work had shown a positive relationship between distal Hox gene dosage and the number of digits, this was exacerbated in the Gli3 null background. Specifically, the number of digits for Hoxa13$^{+/+}$/Hoxd11-13$^{+/+}$/ Gli3$^{-/-}$ mutants was 7–9. Deleting one functional allele of both Hoxa13 and Hoxd11-13 increased this to 8–9, then further to 9–11 when both Hoxd11-13 alleles were removed. Removing another Hoxa13 allele, which left only one distal Hox allele, increased the number of digits to between 12 and 14. The extra digits appeared in limb buds with widths essentially unchanged from the Gli3 null controls. These results were consistent with a computational model based on a simple generic activator–inhibitor system that showed that the number of Turing stripes in a fixed domain is under the control of one of the parameters, which in the case simulated was the activator-dependent production of the inhibitor (Sheth et al., 2012). The authors' conclusion was that the distal Hox genes regulate digit patterning by controlling the wavelength of the pattern produced by a Turing-type mechanism.

While the simulations of Sheth et al. (2012) employed a system of RD equations without assigned chemical identities for the activator and inhibitor, the same group later presented a model based on an identified network of three gene products, namely BMP, Sox9, and Wnt, hence called the BSW model (Raspopovic et al., 2014). While there had been experimental confirmation of only two of the six interactions among the three nodes in this network, the authors were guided by the observation that in vivo, the expression patterns of Wnt and BMP were in phase, and out of phase with Sox9. Mathematically, this constraint indicates that, assuming a RD mechanism, there is an eigenvector for the dominant mode in the linearized system with positive entries for BMP and Wnt, but a negative entry for Sox9. The authors identified a simple network that yields such a pattern. The resulting equations are:

$$\frac{\partial s}{\partial t} = \alpha_s + k_2 b - k_3 w - s^3,$$

$$\frac{\partial b}{\partial t} = \alpha_b - k_4 s - k_5 b + d_b \nabla^2 b,$$

$$\frac{\partial w}{\partial t} = \alpha_w - k_7 s - k_9 w + d_w \nabla^2 w.$$

Here s, b, and w are the concentrations of Sox9, BMP, and Wnt, respectively. The cubic term in the equation of s was introduced to counterbalance the exponential growth of patterns from perturbations of the unstable steady state

and thus induce convergence to a steady-state pattern. Two-dimensional simulations were performed on realistic limb bud-shaped domains, with the Sox9-modulated production rates of BMP and Wnt made dependent on Hoxd13. (These Hoxd13 expression patterns were determined experimentally and mapped onto the simulated limb shapes.) These simulations were in agreement with experiments, including in the case where BMP or Wnt signaling were reduced (Raspopovic et al., 2014).

2.6 | The BMP + BMP receptor model

Badugu et al. (2012) proposed another system of RD equations focusing on the interaction of BMPs and a BMP-receptor as the core network. The corresponding system was modeled by Schnakenberg-type reaction kinetics (Schnakenberg, 1979). The authors included FGF as a third variable that purportedly modulates the production rate of BMPs, based on experimental evidence that FGFs can repress the BMP-antagonist Grem1 (Verheyden & Sun, 2008). (FGF, however, is arguably not a core element of this patterning mechanism, since the FGF-dependent production rate saturates for large FGF concentrations and the BMP/BMP-receptor equations effectively decouple from the FGF equations in this case.) The authors show that the model can produce patterns on realistic limb shapes that agree with experimental results, and identify parameter ranges for which realistic patterning is possible.

A criticism of the BMP/BMP receptor model (see, e.g., Raspopovic et al., 2014) is that the BMP receptor is assumed to freely diffuse with a diffusion coefficient of about one hundredth of that of BMP. As a cell membrane-bound molecule, this receptor does not diffuse in extracellular space, but is passively transported with the cell flux. Thus, a more accurate model would incorporate the cell density as well, and without this, the simplification represented by the BMP/BMP receptor model is difficult to evaluate. However, a separate paper by the same group (Kurics, Menshykau, & Iber, 2014) investigated general RD models based on a freely diffusing ligand and a receptor that only diffuses on the cell surface. The authors simulated the system by partitioning space into subdomains interpreted as cells. They also imposed the condition (motivated by experimental evidence in some systems) that the BMP-BMP receptor complex is positively regulated by the production of the receptor. They then solved RD equations where diffusion of receptors was constrained to each cell with zero-flux conditions, whereas the ligand was allowed to diffuse through intercellular space. In these simulations, Turing patterns still formed, and the Turing space (i.e., the portion of parameter space for which Turing patterns are possible) was enlarged relative to the case where the receptors were allowed to diffuse freely (Kurics et al., 2014).

3 | REFINEMENT AND FINE-TUNING OF THE BASIC SKELETOGENIC MECHANISMS

As we have described in the previous sections, a number of different mathematical models have been proposed for the establishment of chondrogenic condensations based on distinct core morphogenetic networks. The relevant entities in these networks are the gene products that mark early condensations and are thought to mediate their formation, such as BMP receptors, Sox9, or galectins. While these different models may appear to be in conflict with each other, examination of when and where these gene products appear suggests a different viewpoint, namely that these models represent different "modules" in a "skeletogenic toolkit" (Newman et al., 2018). For instance, Newman et al. (2018) point out that the BSW mechanism has only been characterized in the limb autopod, not in more proximal regions (Raspopovic et al., 2014; see also Onimaru, Marcon, Musy, Tanaka, & Sharpe, 2016) and that in in vitro experiments, Sox9 was found not to be necessary for the initial formation of precartilage condensations (Barna & Niswander, 2007). They suggest that the BSW module evolved later than the 2GL mechanism, and possibly the BMP + BMP receptor mechanism, from a separate cell differentiation-inducing module. Stated differently, the BSW network may have originated as a readout of patterns generated by other mechanisms and evolved into a self-organizing system in its own right, contributing robustness to the outcome. This is supported by the finding that the dermal rays of actinopterygians, noncartilaginous structures that do not express Sox9, are nonetheless patterned by mechanisms shared with the tetrapod endoskeleton (Gehrke et al., 2015; Nakamura, Gehrke, Lemberg, Szymaszek, & Shubin, 2016). Similar considerations apply to the TFF network. Although fibronectin is clearly involved in maturation and consolidation of condensations, and TGF-β, in turn, controls fibronectin's (and its own) production, these factors are expressed later in development than, and were possibly superimposed on, galectin- and BMP-dependent networks that evolved in the fins of ancestral fishes (reviewed in Newman et al., 2018).

Thus, different models should not be seen as conflicting explanations in competition with each other as the "true" mechanism, but rather as modules that can act independently, but whose combination imparts extraordinary stability. These ideas are commonplace in developmental biology, but are less appreciated in mathematical modeling. There is strong experimental evidence for local "protocondensations" (Bhat et al., 2011; also termed "compactions" by Barna & Niswander, 2007) of precartilage mesenchyme being fundamental in the development of fin and limb endoskeletons. Similarly, it seems clear that globally acting RD and allied mechanisms function in coordination with this early acting morphogenetic process to pattern the eventual condensations. We now describe two additional mechanisms, one originally proposed prior to the limb-related RD models, and one subsequently, which appear to refine and fine-tune the basic skeletogenic mechanisms.

3.1 | Positional information

One of the most influential ideas in developmental biology has been the conceptual framework of PI, proposed by Lewis Wolpert (Wolpert,1969). This hypothesizes that cells sense their position within the tissue and then, based on this information, execute a position-dependent developmental program, encoded in the organism's genome. PI was suggested to be imparted to the target cells via spatial gradients of certain gene products, that is, morphogens, the same category of secreted components involved in the RD mechanisms described above but employed differently. In the PI scenario, a morphogen is produced by specialized cells in a localized region, spreads by diffusion or directed transport throughout the tissue, thus generating a graded concentration profile. PI itself is embodied in the concentration of the morphogen, which cells respond to based on their evolved interpretative capacities (Wolpert, 1969).

Chemical gradients indeed exist in the developing vertebrate limb bud, most prominently an FGF8 gradient whose source is the AER and which defines the limits of the distal progress zone, and an anterior–posterior gradient of Sonic Hedgehog (Shh). Shh is produced by cells in the posterior region of the limb bud where it meets the body wall, termed the ZPA (see above). The Shh gradient is established by diffusion or active transport (Tickle & Towers, 2017). The ZPA was first discovered through grafting experiments that led to digit duplications (Saunders & Gasseling, 1968), and subsequently conjectured to be the source of a morphogen gradient (Tickle et al., 1975). Later, it was found that Shh was at its highest concentration in the ZPA and that implanting Shh-expressing cells in the limb bud evoked the same digit duplications as ZPA grafting (Riddle, Johnson, Laufer, & Tabin, 1993). Interpreted according to the PI model, Shh was proposed to determine both the number and the different identities of the digits.

However, certain results show that Shh does not have an indispensable role in chondrogenic pattern formation. In both chick and mouse mutants that lack Shh signaling in the limb, the stylopod (i.e., the humerus or femur) and the zeugopod (the fibula and tibia, or the radius and ulna) develop normally, but the number of digits in the autopod is affected (Chiang et al., 2001; Ros et al., 2003). Equally important is the fact that reaggregated limb mesenchymal cells form skeletal elements in reconstituted limb buds in the absence of any ZPA cells (Ros et al., 1994). Strikingly, when the ZPA is deleted along with the transcription factor Gli3, polydactyly results (Litingtung et al., 2002). Thus, Shh's function is not central to the formation of preskeletal condensations, but it has a secondary role in refining the morphology of the autopod. It has thus been argued that a PI mechanism such as the Shh gradient may work in concert with a self-organizing mechanism like the Turing mechanism (Glimm et al., 2012; Green & Sharpe, 2015; Miura, 2013; Raspopovic et al., 2014).

The idea that PI and self-organizing mechanisms are not mutually exclusive is not novel (see for instance Newman, 1988; Wolpert, 1989), but models which explicitly combine the effects of the two are recent. There are, in fact, three formally different ways in which the two mechanisms can interact: either sequentially, with either one downstream from the other, or simultaneously. Mathematically, the most interesting mechanism is the simultaneous variant, with the most plausible connection being that the reaction rates depend on the morphogen concentrations (Borckmans, De Wit, & Dewel, 1992; Glimm et al., 2012; Glimm, Zhang, & Shen, 2009, 2017; Pecze, 2018). For shallow morphogen gradients, the Turing wavenumber is not affected (Glimm et al., 2009), but steep gradients may substantially alter the patterns (Borckmans et al., 1992). In the BSW model (Raspopovic et al., 2014), the interaction of the BSW RD model with an FGF gradient controls the wavelength of the pattern and prevents the distal splitting of digits.

It is now believed that the two roles of Shh postulated by the PI model, the effect on digit number and on digit identity, are independent effects of the morphogen that do not add up to the original proposal of a graded variable specifying digit pattern (Zhu et al., 2008). The endogenous ZPA regulates limb bud width (as mentioned, in coordination with the transcription factor Gli3 (Litingtung et al., 2002)) and, consistent with the primary role of RD processes in

specifying sites of condensation, influences the number of digits. Sonic hedgehog concentration influences digit identity, but in a way that depends on duration of exposure as well as concentration (Harfe et al., 2004) and differs among species (Stewart et al., 2019). The concept of digit identity as a refinement of the primary pattern, possibly by one of the mechanisms described above, is a logical extension of the RD model of skeletogenesis.

3.2 | Morphogenetic field effects via oscillations

Genetic oscillators are common in development. The best studied example is the vertebrate segmentation clock, an oscillatory genetic network that is of central importance in somitogenesis, the process by which the somites, blocks of tissue that generate the vertebral column and associated muscles, form sequentially in pairs along the primary axis in vertebrate embryos (Oates, Morelli, & Ares, 2012). A variant of the so-called clock and wavefront mechanism first proposed by Cooke and Zeeman (1976) appears to be instrumental for somitogenesis. The core idea is the interplay of a molecular clock with a changing state of receptivity of the presomitic mesoderm (PSM) related to its distance from a source of FGF8 at the tail tip. The molecular clock is based on an oscillatory network of genes and gene products, including the Notch receptor and its associated transcriptional coactivator Hes1, with a sector of clock phases permissive to the formation of somites (Hubaud & Pourquié, 2014).

A PDE model of the clock and wavefront mechanism was provided by Collier et al. (2000) with subsequent modifications and elaborations by other authors (e.g., Armstrong et al., 2006; Baker, Schnell, & Maini, 2006; Jörg, Morelli, Soroldoni, Oates, & Jülicher, 2015; see also Baker, Schnell, and Maini (2008) for a survey). For the clock and wavefront model to operate coherently, it is crucial that the clock oscillations are synchronous, that is, that the phases of the molecular oscillators are uniform across the PSM (Jiang et al., 2000; Saga, 2012). The key to establishing and maintaining this synchrony is cell–cell communication, which effectively couples the individual oscillators and leads to synchronization via mutual entrainment, a mathematically well-understood phenomenon (Kuramoto, 1984). The molecular details of the coupling via Notch-dependent intercellular communication in the PSM are also well established (Jiang et al., 2000).

While molecular clocks are also present in limb bud mesenchyme (Pickering et al., 2018; Sheeba, Andrade, & Palmeirim, 2014) they appear to be less important for the core patterning process. However, they appear to play a role in regulating the synchronous appearance of patterns, in effect coordinating pattern formation over spatial ranges that exceed the characteristic distances of morphogen diffusion. Bhat et al. (2019) investigated the role of oscillations in the expression of *hes1*, the gene encoding Hes1. The investigators assayed the expression of *hes1* in cultures of precartilage leg mesenchyme using real-time PCR. Between 12 and 24 hr after plating, this expression was oscillatory, with a period of about 6 hr. This time window coincides with the first appearance of protocondensations. To test the effect of these oscillations on patterning, the authors treated limb micromass cultures with DAPT, which inhibits Notch signaling, and potentially other cell signaling pathways involved in the generation of oscillations. The result was a sustained decrease in *hes1* expression, with no evidence of the oscillations seen in controls. The condensations were found to be markedly less uniform than the control case, indicated by a larger spread of condensation sizes and intercondensational distances (Bhat et al., 2019).

To model the role of Hes1 oscillations mathematically, Bhat et al. (2019) adapted the 2GL model (Glimm et al., 2014) by adding the phase of the *hes1* oscillator as a variable. In this enhanced model, the response of cells to the Gal-1A-mediated adhesion gradients now depends on the *hes1* phase. Effectively, this means that model cells oscillate in a continuous fashion between maximal and minimal responsiveness to the patterning network. A number of scenarios were simulated and compared with experimental results: the *hes1* phase was assumed to be spatially uniform or randomly distributed, and it either oscillated or was constant in time. Simulations in one spatial dimension showed that the absence of spatial uniformity of hes1 phases led to less regular patterns, as seen with DAPT treatment. This was especially pronounced in the case where the *hes1* phase did not oscillate. In contrast, the case of spatially uniform, but nonoscillating phases yielded very similar results to the case of synchronously oscillating phases (Bhat et al., 2019).

These results thus suggest that it is not oscillation per se that is important for the coordination and refinement of condensation formation, but uniform Hes1 status across the tissue field. Synchronized oscillations are an efficient way to achieve such spatial uniformity based on endogenous processes. The simulations also support the view that synchronization of Hes1 oscillation serves as a global coordination mechanism whose spatial range extends beyond the more fundamental core RD mechanism responsible for condensation patterning. Synchrony effectively constitutes the developing tissue as a "morphogenetic field" (in a classic formulation, "a system of order such that the positions taken up by

unstable entities in one part of the system bear a definite relation to the position taken up by other unstable entities in other parts of the system" [Needham, 1937]). While the core 2GL mechanism leads to roughly regular condensation size and spacing, with the superimposed oscillatory mechanism the condensations emerge with a remarkable near-simultaneity and refined pattern geometry (Bhat et al., 2019).

4 | EVOLUTION OF TETRAPOD LIMB PATTERN FORMATION

The structure of the tetrapod limb is highly conserved, with a stereotypical sequence of stylopod (one element: humerus, femur), zeugopod (two elements: radius and ulna, fibula and tibia) and autopod (three to five elements: digits). All tetrapods are descended from members of an earlier-emerging group, the sarcopterygians, that is, lobe-finned fishes. It thus makes sense to study the phylogeny of presumed core chondrogenic patterning motifs to see whether they underwent the kind of key innovation around the origin of the sarcopterygians that may explain the robustness of the tetrapod skeletal limb pattern.

Bhat et al. (2016) undertook such a study for the core 2GL network of the galectins Gal-1 and Gal-8. They compared the Gal-8 sequence between the sarcopterygians, the actinopterygians (ray-finned fishes; a group that contains the vast majority of all fish species) and the chondrichthyans (fishes whose skeletal consists of cartilage, not bone; most prominently, the sharks and rays). They found a deep split in the Gal-8 homologs between actinopterygians on the one hand, and the sarcopterygians and chondrichthyans on the other. The findings indicate that the actinopterygian Gal-8 underwent a translocation, whereas the sarcopterygian Gal-8 retained its synteny. This suggested that the sarcopterygians and chondrichthyans, whose fins or limbs are typically characterized by parallel arrays of endoskeletal elements, and the actinopterygians, whose limbs do not always contain such parallel endoskeletal patterns, may have come to utilize Gal-8 in different ways.

By comparative phylogenomics, the authors also found evidence of purifying selection in the sarcopterygian Gal-8 gene leading to a convergence in the structure of the binding region of the protein it encoded with that of putative chondrogenesis-promoting Gal-1s. This feature, which rendered Gal-8s potentially inhibitory (via competition with a shared counterreceptor) to Gal-1's mediation of protocondensation (a property of the 2GL patterning mechanism), was not seen in actinopterygian Gal-8s (Bhat et al., 2016).

Bhat and coworkers also found strong evidence from comparative phylogenomics that the genes specifying sarcopterygian (but not chondrichthyan or actinopterygian) Gal-8s had acquired *cis*-acting DNA motifs that were potential recognition sites for transcription factors such as Meis1 and Runx2, known to regulate the proximodistal patterning of tetrapod limbs. Using the reduced 2GL model (see section 2.4 above), they investigated the effect of variation in the binding affinity of Gal-8 to its counterreceptor (refinement of which was the plausible target of the observed purifying selection) and the variation in the production rate of Gal-8 (a plausible effect of regulation during limb development of Meis1 and Runx2). They found that the number of elements tends to decrease with increasing production rates of Gal-8 and with increasing binding affinity of Gal-8 to its counterreceptor. Thus, the number of skeletal elements is under fine control of these parameters (Bhat et al., 2016). The rough proximodistal increase in the number of parallel elements in nontetrapod sarcopterygians, and the highly refined species-specific versions of this character throughout the tetrapods, thus appears to be explicable (at least in broad strokes) by the 2GL model (Figure 3, right box).

5 | SUMMARY AND OUTLOOK

Chondrogenic pattern formation in the vertebrate limb has attracted the attention of mathematical modelers for at least 50 years (see for example, Ede & Law, 1969). While until relatively recently, the dominant view was PI-type models in which ("external") temporal or spatial gradients of morphogens were thought to elicit evolved, species-specific programmed responses from the limb bud mesenchymal tissue, more recently, models in which self-organizational ("inherent") capabilities of the mesenchyme itself give rise to patterns have come into greater prominence. Among such models, RD type pattern forming systems are most widely studied, including the BSW model (Raspopovic et al., 2014), the BMP/BMP receptor model (Badugu et al., 2012), the TFF model (Hentschel et al., 2004), as well as the related 2GL model (Glimm et al., 2014). As discussed above, these models should not necessarily be thought of as competing explanations, but rather as representing different patterning modules, with possibly different evolutionary histories, which act sequentially and temporally overlap. We have suggested that the 2GL system, perhaps along with the BMP/BMP

receptor mechanism, were responsible for the initial formation of protocondensations, with the TFF mechanism and, in the autopod, the BSW mechanism locking in and reinforcing the emerging chondrogenic patterns (Newman et al., 2018; Figure 4). These mechanisms operate in a morphogenetic environment in which spatial gradients (such as Shh) and molecular oscillations also have regulatory effects, lending the process additional robustness.

Pattern formation within the developing limb bud entails that mesenchymal cells change their states of determination and differentiation in a spatially dependent fashion. As a cell differentiates, the genes it expresses change and its functional phenotype changes. For this reason, an understanding of transitions among mesenchymal cell states—uncondensed, compacted, condensed, chondrogenic, and apoptotic (defining interelement spaces) will be essential for comprehensive modeling of limb skeletogenesis. In existing models, cell differentiation is represented as a "black box" with addressable type-responses, but this simplification may ultimately prove inadequate for realistic modeling of pattern formation.

Several features of developmental gene regulation resist modeling by conventional mathematical frameworks: lack of stoichiometry and mass action, and changeability of network topology, for example (reviewed in Newman, 2020). This prevents drawing any inferences about the global properties of the regulatory genome of an organism, for example, identifying its attractors with the organism's full array of cell types as has been proposed (Bornholdt & Kauffman, 2019; Kaneko & Yomo, 1999; Kauffman, 1969). Nevertheless, the bi- or tristability properties of Boolean or ordinary differential equation (ODE) networks with small numbers of experimentally relevant variables can serve as good heuristics for studying transitions between cell types that are adjacent to one another in a developmental lineage. The cell types relevant to chondrogenic patterning, discussed in this review (protocondensed and uncondensed mesenchyme, cartilage) fit

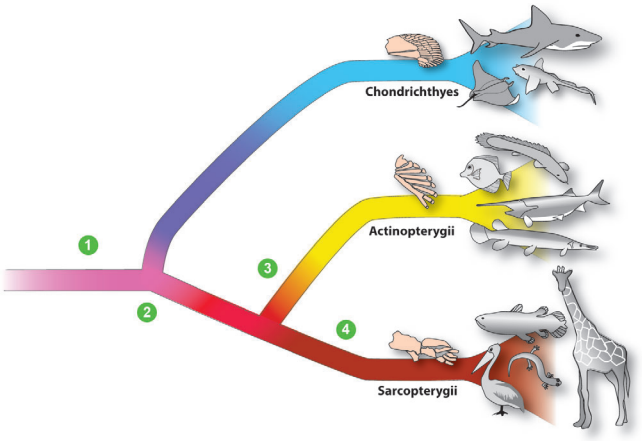

FIGURE 4 Tree showing phylogenetic relationship of extant fish groups and hypothesized appearance of patterning mechanisms. (a) *Capacity for focal cartilage differentiation*. A Gal-1 capable of mediating mesenchymal aggregation was present in ancestral gnathostomes. With the involvement of products of the conserved toolkit genes BMP and BMP receptor 1, and eventually FGF and FGF receptor 2, in expansion-restricting roles, these aggregates would have formed focal compactions or protocondensations. If Sox9 was coordinately induced at these sites they would have been converted to cartilage. Fibronectin, under the regulation of the positive autoregulatory TGF-β, would have consolidated their formation as discrete elements. At some point on this branch of the evolutionary trajectory, a Wnt gene was recruited to the Sox9-BMP couple, forming the BSW Turing-type network, and this would have reinforced the counter-chondrogenic distribution of BMP. Although Gal-8 was present in these organisms, their CRDs had not yet evolved to compete with those of Gal-1, so the full 2GL system was not in place. (b) *Capacity for formation of nodules, stripes, and plates of cartilage*. Evolution of cross-activation of Gal-1 and Gal-8 and of the Gal-8 CRDs to competitive status with Gal-1 CRDs created the 2GL system. This generated numerous parallel cartilage rods and, with fusion, plates. (c) *Variability of the endoskeleton under positive selection*. In the actinopterygians (ray-finned fishes) all the focal chondrogenesis-enabling circuitry was carried forward and (depending on the species), possibly the BSW patterning system (although it appears to be absent in the teleosts; Onimaru et al. (2016)). Selection on the Gal-8 CRD is hypothesized to have reinforced the 2GL patterning circuitry in some, but not all, actinopterygians. (d) *Capacity for regulated proximodistal patterning with small numbers of elements*. In the sarcopterygians (lobe-finned fishes, including tetrapods) the ancestral focal chondrogenesis toolkit and skeletal patterning systems were carried forward, but sometime after their appearance Gal-8 also acquired a unique conserved noncoding, potentially regulatory motif that is hypothesized to have enabled it to be regulated in a quantitative fashion during elongation of the limb bud. This is hypothesized to be the basis of the evolutionarily robust developmental morphology of the tetrapod limb (Bhat et al., 2016). Examples of limb skeletons typical of the various groups are indicated on the respective branches. Source: Based, with modifications, on Newman et al. (2018), fig. 5). CRDs, carbohydrate-recognition domains; 2GL, Two Galectin + Ligands

this criterion. Models for fate specification of lineage-adjacent cell types exist for several developmental processes. These include: early germ layer specification in sea urchins (Bolouri & Davidson, 2002; Kühn et al., 2009; Yuh, Bolouri, & Davidson, 2001), differentiation of the vulval precursor cells in the nematode *Caenorhabditis elegans* (Corson & Siggia, 2012; Giurumescu, Sternberg, & Asthagiri, 2009; Hoyos et al., 2011), and commitment of bone marrow cell precursors (Chickarmane, Enver, & Peterson, 2009; Hong, Oguz, & Tyson, 2015; Salerno, Cosentino, Morrone, & Amato, 2015).

What has largely been neglected in such cell-specification models are interactions between molecules involved in cell patterning and those involved in differentiation. For example, in the case of limb development, the differentiation of mesenchymal cells into cartilage itself occurs a day or more later than the first signs of precartilage condensation (Barna & Niswander, 2007; Frenz et al., 1989,b); however, differences in cell fate trajectories between the cells within condensations and those outside are already observed within early condensations. Specifically, cells within condensations produce the galectins Gal-1A and Gal-8 at much higher rates than those outside (Bhat et al., 2011).

At the core of the 2GL model of Glimm et al. (2014) is the interplay of a regulatory network of the two galectins Gal-1A and Gal-8, with random cell motion biased by Gal-1A mediated cell–cell adhesion. Under the limiting condition of zero cell motility, the 2GL model collapses into a system of only four ODEs. The variables are the concentrations of the galectins and of certain membrane-bound counterreceptors. In preliminary studies, we have observed trajectories in the phase space of this system that either converge to a state in which counterreceptor concentrations and galectin production rates grow exponentially (reflecting the asymptotic state of a cell within a protocondensation), or to a state in which cells lack any counterreceptors (reflecting the state of cells outside condensations). The highly divergent behaviors of these two populations of cells are implicit in the full patterning model, but "tamed" in their expression by the global properties of that system. These nonlinear dynamics may be reflected in the living limb mesenchyme. If so, this would be an unusual case of a pattern formation model providing insight into the molecular mechanisms of differentiation of the constituent cells.

The work we have reviewed suggests a picture in which the current mathematical and computational models of vertebrate limb development remain somewhat fragmented, with each addressing very specific components of the process. Much remains to be done. For instance, including cell densities explicitly in RD models like the BSW network is a crucial next logical step, since pattern formation ultimately requires cell movement. Any patterning mechanism where cell condensation is involved must address the question how the molecular prepattern is translated into a cell density pattern. More generally, there is the question of how chondrogenic patterning interacts with the growth of the limb bud. Notwithstanding substantial modeling of limb bud growth (Boehm et al., 2010; Dillon, Gadgil, & Othmer, 2003; Dillon & Othmer, 1999; Popławski, Swat, Gens, & Glazier, 2007; Suzuki & Morishita, 2017) and of Turing patterns in growing domains (Crampin, Gaffney, & Maini, 1999; Madzvamuse, Maini, & Wathen, 2005; Madzvamuse, Wathen, & Maini, 2003; Miura & Maini, 2004), little work has been done on the effects of growth in the new crop of skeletogenic models. An enhanced degree of realism in future multiscale models should also emerge from studies of how the interplay of two or more pattern forming modules may enhance the robustness of the patterning process, for example, in cases where two RD systems act sequentially to produce a Turing pattern or other developmentally relevant asymmetries (Kinast, Zelnik, Bel, & Meron, 2014).

CONFLICT OF INTEREST

The authors have declared no conflicts of interest for this article.

AUTHOR CONTRIBUTIONS

Tilmann Glimm: T. Glimm: Writing-original draft-equal; writing-review and editing-equal. **Ramray Bhat:** Writing-original draft-equal; writing-review and editing-equal. **Stuart A. Newman:** Writing-original draft-equal; writing-review and editing-equal.

ORCID

Tilmann Glimm https://orcid.org/0000-0003-1040-6509
Ramray Bhat https://orcid.org/0000-0001-6113-4043
Stuart A. Newman https://orcid.org/0000-0002-3569-6429

RELATED WIREs ARTICLES

Establishment of spatial pattern
The benefits differential equations bring to limb development
Oscillatory gene expression and somitogenesis

The Sonic hedgehog gradient in the developing limb
Module-based complexity formation: periodic patterning in feathers and hairs

FURTHER READING

Chatterjee, P., Glimm, T. & Kazmierczak, B. (2020). Mathematical modeling of chondrogenic pattern formation during limb development: Recent advances in continuous models. *Mathematical Biosciences 322*, 108319.

REFERENCES

Ahrens, P. B., Solursh, M., & Reiter, R. S. (1977). Stage-related capacity for limb chondrogenesis in cell culture. *Developmental Biology*, *60*, 69–82.

Alber, M., Glimm, T., Hentschel, H. G. E., Kazmierczak, B., Zhang, Y.-T., Zhu, J., & Newman, S. A. (2008). The morphostatic limit for a model of skeletal pattern formation in the vertebrate limb. *Bulletin of Mathematical Biology*, *70*, 460–483.

Alber, M., Hentschel, H. G. E., Kazmierczak, B., & Newman, S. A. (2005). Existence of solutions to a new model of biological pattern formation. *Journal of Mathematical Analysis and Applications*, *308*, 175–194.

Armstrong, N. J., Painter, K. J., & Sherratt, J. A. (2006). A continuum approach to modelling cell–cell adhesion. *Journal of Theoretical Biology*, *243*, 98–113.

Badugu, A., Kraemer, C., Germann, P., Menshykau, D., & Iber, D. (2012). Digit patterning during limb development as a result of the BMP-receptor interaction. *Scientific Reports*, *2*, 991.

Baker, R. E., Schnell, S., & Maini, P. K. (2006). A clock and wavefront mechanism for somite formation. *Developmental Biology*, *293*, 116–126.

Baker, R. E., Schnell, S., & Maini, P. K. (2008). Mathematical models for somite formation. *Current Topics in Developmental Biology*, *81*, 183–203.

Barna, M., & Niswander, L. (2007). Visualization of cartilage formation: Insight into cellular properties of skeletal progenitors and chondrodysplasia syndromes. *Developmental Cell*, *12*, 931–941.

Bhat, R., Chakraborty, M., Glimm, T., Stewart, T. A., & Newman, S. A. (2016). Deep phylogenomics of a tandem-repeat galectin regulating appendicular skeletal pattern formation. *BMC Evolutionary Biology*, *16*, 162.

Bhat, R., Chakraborty, M., Mian, I. S., & Newman, S. A. (2014). Structural divergence in vertebrate phylogeny of a duplicated prototype galectin. *Genome Biology and Evolution*, *6*, 2721–2730.

Bhat, R., Glimm, T., Linde-Medina, M., Cui, C., & Newman, S. A. (2019). Synchronization of Hes1 oscillations coordinates and refines condensation formation and patterning of the avian limb skeleton. *Mechanisms of Development*, *156*, 41–54.

Bhat, R., Lerea, K. M., Peng, H., Kaltner, H., Gabius, H. J., & Newman, S. A. (2011). A regulatory network of two galectins mediates the earliest steps of avian limb skeletal morphogenesis. *BMC Developmental Biology*, *11*, 6.

Boehm, B., Westerberg, H., Lesnicar-Pucko, G., Raja, S., Rautschka, M., Cotterell, J., ... Sharpe, J. (2010). The role of spatially controlled cell proliferation in limb bud morphogenesis. *PLoS Biology*, *8*, e1000420.

Bolouri, H., & Davidson, E. H. (2002). Modeling DNA sequence-based *cis*-regulatory gene networks. *Developmental Biology*, *246*, 2–13.

Borckmans, A., De Wit, A., & Dewel, G. (1992). Competition in ramped Turing structures. *Physica A*, *188*, 137–157.

Bornholdt, S., & Kauffman, S. (2019). Ensembles, dynamics, and cell types: Revisiting the statistical mechanics perspective on cellular regulation. *Journal of Theoretical Biology*, *467*, 15–22.

Chaturvedi, R., Huang, C., Kazmierczak, B., Schneider, T., Izaguirre, J. A., Glimm, T., ... Alber, M. S. (2005). On multiscale approaches to three-dimensional modelling of morphogenesis. *Journal of the Royal Society, Interface*, *2*, 237–253.

Chiang, C., Litingtung, Y., Harris, M. P., Simandl, B. K., Li, Y., Beachy, P. A., & Fallon, J. F. (2001). Manifestation of the limb prepattern: Limb development in the absence of sonic hedgehog function. *Developmental Biology*, *236*, 421–435.

Chickarmane, V., Enver, T., & Peterson, C. (2009). Computational modeling of the hematopoietic erythroid–myeloid switch reveals insights into cooperativity, priming, and irreversibility. *PLoS Computational Biology*, *5*, e1000268.

Christley, S., Alber, M. S., & Newman, S. A. (2007). Patterns of mesenchymal condensation in a multiscale, discrete stochastic model. *PLoS Computational Biology*, *3*, e76.

Cickovski, T. M., Huang, C., Chaturvedi, R., Glimm, T., Hentschel, H. G., Alber, M. S., ... Izaguirre, J. A. (2005). A framework for three-dimensional simulation of morphogenesis. *IEEE/ACM Transactions on Computational Biology and Bioinformatics*, *2*, 273–288.

Collier, J. R., Mcinerney, D., Schnell, S., Maini, P. K., Gavaghan, D. J., Houston, P., & Stern, C. D. (2000). A cell cycle model for somitogenesis: Mathematical formulation and numerical simulation. *Journal of Theoretical Biology*, *207*, 305–316.

Cooke, J., & Zeeman, E. C. (1976). A clock and wavefront model for control of the number of repeated structures during animal morphogenesis. *Journal of Theoretical Biology*, *58*, 455–476.

Corson, F., & Siggia, E. D. (2012). Geometry, epistasis, and developmental patterning. *Proceedings of the National Academy of Sciences of the United States of America*, *109*, 5568–5575.

Crampin, E. J., Gaffney, E. A., & Maini, P. K. (1999). Reaction and diffusion on growing domains: Scenarios for robust pattern formation. *Bulletin of Mathematical Biology*, *61*, 1093–1120.

De Lise, A. M., Stringa, E., Woodward, W. A., Mello, M. A., & Tuan, R. S. (2000). Embryonic limb mesenchyme micromass culture as an in vitro model for chondrogenesis and cartilage maturation. In R. S. Tuan & C. W. Lo (Eds.), *Developmental biology protocols: Methods in molecular biology* (pp. 359–375). Totowa, NJ: Humana Press.

Diekmann, O., 1999. Modeling and analysing physiologically structured populations, in: *Mathematics inspired by biology (Martina Franca, 1997), Lecture Notes in Mathematics*. Springer, Berlin, pp. 1–37.

Dillon, R., Gadgil, C., & Othmer, H. G. (2003). Short- and long-range effects of sonic hedgehog in limb development. *Proceedings of the National Academy of Sciences of the United States of America*, *100*, 10152–10157.

Dillon, R., & Othmer, H. G. (1999). A mathematical model for outgrowth and spatial patterning of the vertebrate limb bud. *Journal of Theoretical Biology*, *197*, 295–330.

Downie, S. A., & Newman, S. A. (1994). Morphogenetic differences between fore and hind limb precartilage mesenchyme: Relation to mechanisms of skeletal pattern formation. *Developmental Biology*, *162*, 195–208.

Dudley, A. T., Ros, M. A., & Tabin, C. J. (2002). A re-examination of proximodistal patterning during vertebrate limb development. *Nature*, *418*, 539–544.

Ede, D. A., & Law, J. T. (1969). Computer simulation of vertebrate limb morphogenesis. *Nature*, *221*, 244–248.

Frenz, D. A., Akiyama, S. K., Paulsen, D. F., & Newman, S. A. (1989). Latex beads as probes of cell surface-extracellular matrix interactions during chondrogenesis: Evidence for a role for amino-terminal heparin-binding domain of fibronectin. *Developmental Biology*, *136*, 87–96.

Frenz, D. A., Jaikaria, N. S., & Newman, S. A. (1989). The mechanism of precartilage mesenchymal condensation: A major role for interaction of the cell surface with the amino-terminal heparin-binding domain of fibronectin. *Developmental Biology*, *136*, 97–103.

Gehrke, A. R., Schneider, I., de la Calle-Mustienes, E., Tena, J. J., Gomez-Marin, C., Chandran, M., … Shubin, N. H. (2015). Deep conservation of wrist and digit enhancers in fish. *Proceedings of the National Academy of Sciences*, *112*, 803–808.

Giurumescu, C. A., Sternberg, P. W., & Asthagiri, A. R. (2009). Predicting phenotypic diversity and the underlying quantitative molecular transitions. *PLoS Computational Biology*, *5*, e1000354.

Glazier, J. A., & Graner, F. (1993). Simulation of the differential adhesion driven rearrangement of biological cells. *Physical Review E: Statistical Physics, Plasmas, Fluids, and Related Interdisciplinary Topics*, *47*, 2128–2154.

Glimm, T., Bhat, R., & Newman, S. A. (2014). Modeling the morphodynamic galectin patterning network of the developing avian limb skeleton. *Journal of Theoretical Biology*, *346*, 86–108.

Glimm, T., Headon, D., & Kiskowski, M. A. (2012). Computational and mathematical models of chondrogenesis in vertebrate limbs. *Birth Defects Research. Part C, Embryo Today*, *96*, 176–192.

Glimm, T., Zhang, J., Shen, Y.-Q., & Newman, S. A. (2012). Reaction–diffusion systems and external morphogen gradients: The two-dimensional case, with an application to skeletal pattern formation. *Bulletin of Mathematical Biology*, *74*, 666–687.

Glimm, T., Zhang, J., & Shen, Y.-Q. (2009). Interaction of Turing patterns with an external linear morphogen gradient. *Nonlinearity*, *22*, 2541–2560.

Glimm, T., Zhang, J., & Shen, Y.-Q. (2017). Stability of Turing-type patterns in a reaction–diffusion system with an external gradient. *International Journal of Bifurcation and Chaos*, *27*, 1750003.

Green, J. B. A., & Sharpe, J. (2015). Positional information and reaction-diffusion: Two big ideas in developmental biology combine. *Development*, *142*, 1203–1211.

Grigorian, A., & Demetriou, M. (2010). Manipulating cell surface glycoproteins by targeting *N*-glycan-galectin interactions. *Methods in Enzymology*, *480*, 245–266.

Hamburger, V., & Hamilton, H. L. (1951). A series of normal stages in the development of the chick embryo. *Journal of Morphology*, *88*, 49–92.

Harfe, B. D., Scherz, P. J., Nissim, S., Tian, H., McMahon, A. P., & Tabin, C. J. (2004). Evidence for an expansion-based temporal Shh gradient in specifying vertebrate digit identities. *Cell*, *118*, 517–528.

Harris, A. K., Stopak, D., & Warner, P. (1984). Generation of spatially periodic patterns by a mechanical instability: A mechanical alternative to the Turing model. *Journal of Embryology and Experimental Morphology*, *80*, 1–20.

Harris, A. K., Stopak, D., & Wild, P. (1981). Fibroblast traction as a mechanism for collagen morphogenesis. *Nature*, *290*, 249–251.

Hentschel, H. G. E., Glimm, T., Glazier, J. A., & Newman, S. A. (2004). Dynamical mechanisms for skeletal pattern formation in the vertebrate limb. *Proceedings of the Royal Society of London. Series B: Biological Sciences*, *271*, 1713–1722.

Hong, T., Oguz, C., & Tyson, J. J. (2015). A mathematical framework for understanding four-dimensional heterogeneous differentiation of CD4+ T cells. *Bulletin of Mathematical Biology*, *77*, 1046–1064.

Hoyos, E., Kim, K., Milloz, J., Barkoulas, M., Pénigault, J.-B., Munro, E., & Félix, M.-A. (2011). Quantitative variation in autocrine signaling and pathway crosstalk in the Caenorhabditis vulva network. *Current Biology CB*, *21*, 527–538.

Hubaud, A., & Pourquié, O. (2014). Signalling dynamics in vertebrate segmentation. *Nature Reviews. Molecular Cell Biology*, *15*, 709–721.

Iber, D., & Zeller, R. (2012). Making sense-data-based simulations of vertebrate limb development. *Current Opinion in Genetics & Development*, *22*, 570–577.

Jiang, Y. J., Aerne, B. L., Smithers, L., Haddon, C., Ish-Horowicz, D., & Lewis, J. (2000). Notch signalling and the synchronization of the somite segmentation clock. *Nature*, *408*, 475–479.

Jörg, D. J., Morelli, L. G., Soroldoni, D., Oates, A. C., & Jülicher, F. (2015). Continuum theory of gene expression waves during vertebrate segmentation. *New Journal of Physics*, *17*, 093042.

Kaneko, K., & Yomo, T. (1999). Isologous diversification for robust development of cell society. *Journal of Theoretical Biology*, *199*, 243–256.

Kauffman, S. A. (1969). Metabolic stability and epigenesis in randomly constructed genetic nets. *Journal of Theoretical Biology*, *22*, 437–467.

Kinast, S., Zelnik, Y. R., Bel, G., & Meron, E. (2014). Interplay between Turing mechanisms can increase pattern diversity. *Physical Review Letters*, *112*, 078701.

Kiskowski, M. A., Alber, M. S., Thomas, G. L., Glazier, J. A., Bronstein, N. B., Pu, J., & Newman, S. A. (2004). Interplay between activator-inhibitor coupling and cell-matrix adhesion in a cellular automaton model for chondrogenic patterning. *Developmental Biology*, *271*, 372–387.

Kühn, C., Wierling, C., Kühn, A., Klipp, E., Panopoulou, G., Lehrach, H., & Poustka, A. J. (2009). Monte Carlo analysis of an ODE model of the sea urchin endomesoderm network. *BMC Systems Biology*, *3*, 83.

Kuramoto, Y. (1984). *Chemical oscillations, waves, and turbulence*. Berlin, Heidelberg: Springer Verlag.

Kurics, T., Menshykau, D., & Iber, D. (2014). Feedback, receptor clustering, and receptor restriction to single cells yield large Turing spaces for ligand-receptor-based Turing models. *Physical Review E*, *90*, 022716.

Leonard, C. M., Fuld, H. M., Frenz, D. A., Downie, S. A., Massagué, J., & Newman, S. A. (1991). Role of transforming growth factor-β in chondrogenic pattern formation in the embryonic limb: Stimulation of mesenchymal condensation and fibronectin gene expression by exogenous TGF-β and evidence for endogenous TGF-β-like activity. *Developmental Biology*, *145*, 99–109.

Lewis, C. A., Pratt, R. M., Pennypacker, J. P., & Hassell, J. R. (1978). Inhibition of limb chondrogenesis in vitro by vitamin A: Alterations in cell surface characteristics. *Developmental Biology*, *64*, 31–47.

Li, Y., Toole, B. P., Dealy, C. N., & Kosher, R. A. (2007). Hyaluronan in limb morphogenesis. *Developmental Biology*, *305*, 411–420.

Litingtung, Y., Dahn, R. D., Li, Y., Fallon, J. F., & Chiang, C. (2002). Shh and Gli3 are dispensable for limb skeleton formation but regulate digit number and identity. *Nature*, *418*, 979–983.

Madzvamuse, A., Maini, P. K., & Wathen, A. J. (2005). A moving grid finite element method for the simulation of pattern generation by Turing models on growing domains. *Journal of Scientific Computing*, *24*, 247–262.

Madzvamuse, A., Wathen, A. J., & Maini, P. K. (2003). A moving grid finite element method applied to a model biological pattern generator. *Journal of Computational Physics*, *190*, 478–500.

Maini, P. K., & Solursh, M. (1991). Cellular mechanisms of pattern formation in the developing limb. *International Review of Cytology*, *129*, 91–133.

Marcon, L., Diego, X., Sharpe, J., & Muller, P. (2016). High-throughput mathematical analysis identifies Turing networks for patterning with equally diffusing signals. *eLife*, *5*, e14022. https://doi.org/10.7554/eLife.14022.

Mariani, F. V., & Martin, G. R. (2003). Deciphering skeletal patterning: Clues from the limb. *Nature*, *423*, 319–325.

Meinhardt, H., & Gierer, A. (2000). Pattern formation by local self-activation and lateral inhibition. *BioEssays: News and Reviews in Molecular, Cellular and Developmental Biology*, *22*, 753–760.

Metz, J. A., & Diekmann, O. (1986). *The dynamics of physiologically structured populations*. Berlin, Heidelberg: Springer.

Miura, T. (2013). Turing and Wolpert work together during limb development. *Science Signaling*, *6*, pe14.

Miura, T., & Maini, P. K. (2004). Speed of pattern appearance in reaction-diffusion models: Implications in the pattern formation of limb bud mesenchyme cells. *Bulletin of Mathematical Biology*, *66*, 627–649.

Miura, T., Shiota, K., Morriss-Kay, G., & Maini, P. K. (2006). Mixed-mode pattern in Double foot mutant mouse limb–Turing reaction-diffusion model on a growing domain during limb development. *Journal of Theoretical Biology*, *240*, 562–573.

Mochizuki, A., Wada, N., Ide, H., & Iwasa, Y. (1998). Cell-cell adhesion in limb-formation, estimated from photographs of cell sorting experiments based on a spatial stochastic model. *Developmental Dynamics*, *211*, 204–214.

Moftah, M. Z., Downie, S. A., Bronstein, N. B., Mezentseva, N., Pu, J., Maher, P. A., & Newman, S. A. (2002). Ectodermal FGFs induce perinodular inhibition of limb chondrogenesis in vitro and in vivo via FGF receptor 2. *Developmental Biology*, *249*, 270–282.

Murray, J. D. (2002). *Mathematical biology II: Interdisciplinary Applied Mathematics* (3rd. ed.). New York: Springer-Verlag.

Nakamura, T., Gehrke, A. R., Lemberg, J., Szymaszek, J., & Shubin, N. H. (2016). Digits and fin rays share common developmental histories. *Nature*, *537*, 225–228.

Needham, J. (1937). Chemical aspects of morphogenetic fields. In J. Needham & D. E. Green (Eds.), *Perspectives in biochemistry* (pp. 66–80). London: Cambridge University Press.

Newman, S. A. (1988). Lineage and pattern in the developing vertebrate limb. *Trends in Genetics*, *4*, 329–332.

Newman, S. A. (1996). Sticky fingers: Hox genes and cell adhesion in vertebrate limb development. *BioEssays*, *18*, 171–174.

Newman, S. A. (2007). The Turing mechanism in vertebrate limb patterning. *Nature Reviews. Molecular Cell Biology*, *8*, 1. https://doi.org/10.1038/nrm1830-c1

Newman, S. A. (2020). Cell differentiation: What have we learned in 50 years? *Journal of Theoretical Biology*, *485*, 11031.

Newman, S. A., & Bhat, R. (2007). Activator-inhibitor dynamics of vertebrate limb pattern formation. *Birth Defects Research Part C: Embryo Today*, *81*, 305–319.

Newman, S. A., & Frisch, H. L. (1979). Dynamics of skeletal pattern formation in developing chick limb. *Science*, *205*, 662–668.

Newman, S. A., Frisch, H. L., & Percus, J. K. (1988). On the stationary state analysis of reaction-diffusion mechanisms for biological pattern formation. *Journal of Theoretical Biology*, *134*, 183–197.

Newman, S. A., Glimm, T., & Bhat, R. (2018). The vertebrate limb: An evolving complex of self-organizing systems. *Progress in Biophysics and Molecular Biology*, *137*, 12–24.

Newman, S. A., & Müller, G. B. (2005). Origination and innovation in the vertebrate limb skeleton: An epigenetic perspective. *Journal of Experimental Zoology. Part B, Molecular and Developmental Evolution*, *304*, 593–609.

Oates, A. C., Morelli, L. G., & Ares, S. (2012). Patterning embryos with oscillations: Structure, function and dynamics of the vertebrate segmentation clock. *Development*, *139*, 625–639.

Onimaru, K., Marcon, L., Musy, M., Tanaka, M., & Sharpe, J. (2016). The fin-to-limb transition as the re-organization of a Turing pattern. *Nature Communications*, *7*, 11582.

Oster, G. F., Murray, J. D., & Harris, A. K. (1983). Mechanical aspects of mesenchymal morphogenesis. *Development*, *78*, 83–125.

Oster, G. F., Murray, J. D., & Maini, P. K. (1985). A model for chondrogenic condensations in the developing limb: The role of extracellular matrix and cell tractions. *Journal of Embryology and Experimental Morphology*, *89*, 93–112.

Pecze, L. (2018). A solution to the problem of proper segment positioning in the course of digit formation. *Biosystems, Computational, Theoretical, and Experimental Approaches to Morphogenesis*, *173*, 266–272.

Pickering, J., Rich, C. A., Stainton, H., Aceituno, C., Chinnaiya, K., Saiz-Lopez, P., ... Towers, M. (2018). An intrinsic cell cycle timer terminates limb bud outgrowth. *eLife*, *7*, e37429. https://doi.org/10.7554/eLife.37429.

Popławski, N. J., Swat, M., Gens, J. S., & Glazier, J. A. (2007). Adhesion between cells, diffusion of growth factors, and elasticity of the AER produce the paddle shape of the chick limb. *Physica A*, *373*, 521–532.

Raspopovic, J., Marcon, L., Russo, L., & Sharpe, J. (2014). Modeling digits. Digit patterning is controlled by a bmp-Sox9-Wnt Turing network modulated by morphogen gradients. *Science*, *345*, 566–570.

Riddle, R. D., Johnson, R. L., Laufer, E., & Tabin, C. (1993). Sonic hedgehog mediates the polarizing activity of the ZPA. *Cell*, *75*, 1401–1416.

Roberts, C. J., Birkenmeier, T. M., McQuillan, J. J., Akiyama, S. K., Yamada, S. S., Chen, W. T., ... McDonald, J. A. (1988). Transforming growth factor beta stimulates the expression of fibronectin and of both subunits of the human fibronectin receptor by cultured human lung fibroblasts. *The Journal of Biological Chemistry*, *263*, 4586–4592.

Ros, M. A., Dahn, R. D., Fernandez-Teran, M., Rashka, K., Caruccio, N. C., Hasso, S. M., ... Fallon, J. F. (2003). The chick oligozeugodactyly (ozd) mutant lacks sonic hedgehog function in the limb. *Development*, *130*, 527–537.

Ros, M. A., Lyons, G. E., Mackem, S., & Fallon, J. F. (1994). Recombinant limbs as a model to study Homeobox gene regulation during limb development. *Developmental Biology*, *166*, 59–72.

Saga, Y. (2012). The synchrony and cyclicity of developmental events. *Cold Spring Harbor Perspectives in Biology*, *4*, a008201.

Salazar-Ciudad, I., Jernvall, J., & Newman, S. A. (2003). Mechanisms of pattern formation in development and evolution. *Development*, *130*, 2027–2037.

Salerno, L., Cosentino, C., Morrone, G., & Amato, F. (2015). Computational modeling of a transcriptional switch underlying B-lymphocyte lineage commitment of hematopoietic multipotent cells. *PLoS One*, *10*, e0132208.

Saunders, J. W., Jr. (1948). The proximo-distal sequence of origin of the parts of the chick wing and the role of the ectoderm. *The Journal of Experimental Zoology*, *108*, 363–402.

Saunders, J. W., Jr., & Gasseling, M. (1968). Ectodermal–mesenchymal interactions in the origin of limb symmetry. In R. Fleischmajer & R. Billingham (Eds.), *Epithelial–Mesenchymal interactions* (pp. 78–97). Baltimore: Williams & Wilkins.

Saunders, J. W. (2002). Is the Progress Zone Model a Victim of Progress? *Cell*, *110*, 541–543.

Schnakenberg, J. (1979). Simple chemical reaction systems with limit cycle behaviour. *Journal of Theoretical Biology*, *81*, 389–400.

Sheeba, C. J., Andrade, R. P., & Palmeirim, I. (2014). Limb patterning: From signaling gradients to molecular oscillations. *Journal of Molecular Biology*, *426*, 780–784.

Sheth, R., Marcon, L., Bastida, M. F., Junco, M., Quintana, L., Dahn, R., ... Ros, M. A. (2012). Hox genes regulate digit patterning by controlling the wavelength of a Turing-type mechanism. *Science*, *338*, 1476–1480.

Silver, M. H., Foidart, J. M., & Pratt, R. M. (1981). Distribution of fibronectin and collagen during mouse limb and palate development. *Differentiation*, *18*, 141–149.

Steinberg, M. S. (2007). Differential adhesion in morphogenesis: A modern view. *Current Opinion in Genetics and Development*, *17*, 281–286.

Stewart, T. A., Bhat, R., & Newman, S. A. (2017). The evolutionary origin of digit patterning. *EvoDevo*, *8*, 21.

Stewart, T. A., Liang, C., Cotney, J. L., Noonan, J. P., Sanger, T. J., & Wagner, G. P. (2019). Evidence against tetrapod-wide digit identities and for a limited frame shift in bird wings. *Nature Communications*, *10*, 1–13.

Summerbell, D., Lewis, J. H., & Wolpert, L. (1973). Positional Information in Chick Limb Morphogenesis. *Nature*, *244*, 492–496.

Summerbell, D. (1976). A descriptive study of the rate of elongation and differentiation of the skeleton of the developing chick wing. *Journal of Embryology and Experimental Morphology*, *35*, 241–260.

Suzuki, T., & Morishita, Y. (2017). A quantitative approach to understanding vertebrate limb morphogenesis at the macroscopic tissue level. *Current Opinion in Genetics & Development*, *45*, 108–114. https://doi.org/10.1016/j.gde.2017.04.005.

Szebenyi, G., Savage, M. P., Olwin, B. B., & Fallon, J. F. (1995). Changes in the expression of fibroblast growth factor receptors mark distinct stages of chondrogenesis in vitro and during chick limb skeletal patterning. *Developmental Dynamics*, *204*, 446–456.

Thieme, H. R. (2003). *Mathematics in population biology, Princeton series in theoretical and computational biology*. Princeton, NJ: Princeton University Press.

Tickle, C. (2003). Patterning systems—from one end of the limb to the other. *Developmental Cell*, *4*, 449–458.

Tickle, C., Summerbell, D., & Wolpert, L. (1975). Positional signalling and specification of digits in chick limb morphogenesis. *Nature*, *254*, 199–202.

Tickle, C., & Towers, M. (2017). Sonic hedgehog signaling in limb development. *Frontiers in Cell and Development Biology*, *5*. https://doi.org/10.3389/fcell.2017.00014.

Tomasek, J. J., Mazurkiewicz, J. E., & Newman, S. A. (1982). Nonuniform distribution of fibronectin during avian limb development. *Developmental Biology*, *90*, 118–126.

Turing, A. M. (1952). The chemical basis of morphogenesis. *Philosophical Transactions of the Royal Society B*, *237*, 37–72.

Van Obberghen-Schilling, E., Roche, N. S., Flanders, K. C., Sporn, M. B., & Roberts, A. B. (1988). Transforming growth factor beta 1 positively regulates its own expression in normal and transformed cells. *The Journal of Biological Chemistry*, *263*, 7741–7746.

Verheyden, J. M., & Sun, X. (2008). An Fgf/Gremlin inhibitory feedback loop triggers termination of limb bud outgrowth. *Nature*, *454*, 638–641.

Wolpert, L. (1969). Positional information and the spatial pattern of cellular differentiation. *Journal of Theoretical Biology*, *25*, 1–47.

Wolpert, L. (1989). Positional information revisited. *Development*, *107*(Suppl), 3–12.

Woolley, T. E., Baker, R. E., Tickle, C., Maini, P. K., & Towers, M. (2014). Mathematical modelling of digit specification by a sonic hedgehog gradient. *Developmental Dynamics*, *243*, 290–298.

Yokouchi, Y., Nakazato, S., Yamamoto, M., Goto, Y., Kameda, T., Iba, H., & Kuroiwa, A. (1995). Misexpression of Hoxa-13 induces cartilage homeotic transformation and changes cell adhesiveness in chick limb buds. *Genes & Development*, *9*, 2509–2522.

Yuh, C. H., Bolouri, H., & Davidson, E. H. (2001). Cis-regulatory logic in the endo16 gene: Switching from a specification to a differentiation mode of control. *Development*, *128*, 617–629.

Zeng, W., Thomas, G. L., & Glazier, J. A. (2004). Non-Turing stripes and spots: A novel mechanism for biological cell clustering. *Physica A: Statistical Mechanics and its Applications*, *341*, 482–494.

Zeng, W., Thomas, G. L., Newman, S. A., & Glazier, J. A. (2002). A novel mechanism for mesenchymal condensation during limb chondrogenesis in vitro. In *Mathematical Modelling and computing in biology and medicine, 5th ESMTB conference* (pp. 80–86). Bologna: Esculapio.

Zhang, Y. T., Alber, M. S., & Newman, S. A. (2012). Mathematical modeling of vertebrate limb development. *Mathematical Biosciences*, *243*, 1–17.

Zhu, J., Nakamura, E., Nguyen, M.-T., Bao, X., Akiyama, H., & Mackem, S. (2008). Uncoupling sonic hedgehog control of pattern and expansion of the developing limb bud. *Developmental Cell*, *14*, 624–632.

Zhu, J., Zhang, Y. T., Alber, M. S., & Newman, S. A. (2010). Bare bones pattern formation: A core regulatory network in varying geometries reproduces major features of vertebrate limb development and evolution. *PLoS One*, *5*, e10892.

Zhu, J., Zhang, Y.-T., Newman, S. A., & Alber, M. S. (2009). A finite element model based on discontinuous Galerkin methods on moving grids for vertebrate limb pattern formation. *Mathematical Modelling of Natural Phenomena*, *4*, 131–148.

Zwilling, E. (1964). Development of fragmented and of dissociated limb bud mesoderm. *Developmental Biology*, *89*, 20–37.

How to cite this article: Glimm T, Bhat R, Newman SA. Multiscale modeling of vertebrate limb development. *WIREs Syst Biol Med*. 2020;e1485. https://doi.org/10.1002/wsbm.1485